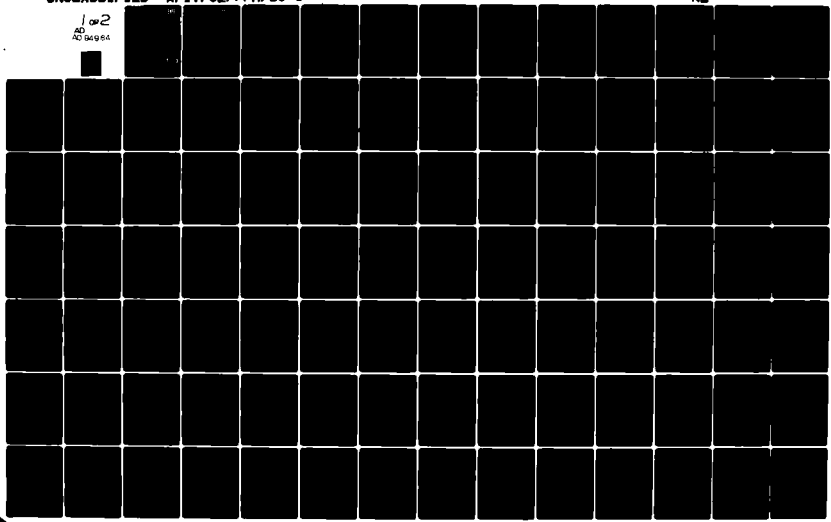


AD-A094 964 AIR FORCE INST OF TECH WRIGHT-PATTERSON AFB OH SCHOO--ETC F/8 7/4
A GAS FLOW TUBE FOR SPECTROSCOPIC STUDIES. (U)
DEC 80 V R KOYM
AFIT/GEF/PH/80-5

UNCLASSIFIED

NL

1 of 2
AS
NOV 84

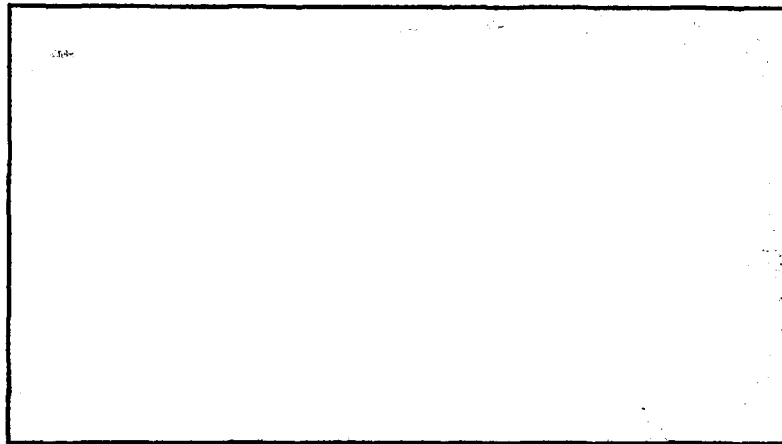


① LEVEL IV

AIR FORCE INSTITUTE OF TECHNOLOGY



AIR UNIVERSITY
UNITED STATES AIR FORCE



SCHOOL OF ENGINEERING

DTIC
ELECTE
FEB 12 1981

S D

B

WRIGHT-PATTERSON AIR FORCE BASE, OHIO

DTIC FILE COPY

DISTRIBUTION STATEMENT A
Approved for public release;
Distribution Unlimited

81 2 02 161

① LEVEL 2

AFIT/GEP/PH/80-5

14 JAN 1981

APPROVED FOR PUBLIC RELEASE AFR 190-17.

Fredric C. Lynch
FREDRIC C. LYNCH, Major, USAF
Director of Public Affairs
Air Force Institute of Technology (ATC)
Wright-Patterson AFB, OH 45433

A GAS FLOW TUBE
FOR SPECTROSCOPIC STUDIES

THESIS

AFIT/GEP/PH/80-5

Vernon R. Koym
Capt USAF

DTIC
ELECTE
S FEB 12 1981 D
B

Approved for public release; distribution unlimited.

AFIT/GEP/PH/80-5

A GAS FLOW TUBE
FOR SPECTROSCOPIC STUDIES

THESIS,

Presented to the Faculty of the School of Engineering
of the Air Force Institute of Technology
Air University
in Partial Fulfillment of the
Requirements for the Degree of
Master of Science

by

Vernon R. Koym / B.S.

Capt USAF

Graduate Engineering Physics

Dec ~~1980~~ 1980

Approved for public release; distribution unlimited.

Contents

| | <u>Page</u> |
|---------------------------------------|-------------|
| Preface----- | ii |
| List of Figures----- | v |
| List of Tables----- | vii |
| List of Symbols----- | viii |
| Abstract----- | xii |
| I. Introduction----- | 1 |
| Background----- | 1 |
| Objective----- | 3 |
| General Approach----- | 3 |
| II. Theory----- | 5 |
| Introduction----- | 5 |
| Background----- | 5 |
| I ₂ Chemiluminescence----- | 8 |
| PbO Reaction----- | 9 |
| Singlet Molecular Oxygen----- | 11 |
| Gas Flow Tubes----- | 14 |
| III. Experimental Apparatus----- | 24 |
| Introduction----- | 24 |
| Flow Tube----- | 24 |
| Vapor Generation----- | 33 |
| Ancillary Equipment----- | 37 |
| IV. Experimental Procedure----- | 40 |
| Introduction----- | 40 |
| Alignment and Calibration----- | 40 |
| Data Collection----- | 43 |
| Safety----- | 45 |
| V. Results and Discussion----- | 46 |
| Gas Flow Tube Performance----- | 46 |
| I ₂ Experiment----- | 51 |
| PbO Experiment----- | 62 |

Contents (Cont'd)

| | <u>Page</u> |
|---|-------------|
| VI. Conclusions and Recommendations----- | 64 |
| Flow Tube Performance----- | 64 |
| Experiments----- | 64 |
| Recommendations----- | 65 |
| Possible Investigations----- | 69 |
| Bibliography----- | 74 |
| Appendix A: Flow Tube Procedure----- | 80 |
| Appendix B: Pictures of Apparatus----- | 83 |
| Appendix C: Useful PbO Data----- | 85 |
| Appendix D: Response Curves for Photomultiplier Tubes----- | 88 |
| Vita----- | 91 |

List of Figures

| <u>Figure</u> | | <u>Page</u> |
|---------------|---|-------------|
| 1 | I ₂ /O ₂ Energy Levels----- | 7 |
| 2 | O ₂ Potential Curves----- | 12 |
| 3 | Recirculation A+A _n Expansion Point----- | 15 |
| 4 | Velocity Profiles Under the Turbulent, Laminar, and Plug Flow Regimes----- | 19 |
| 5 | Experimental Apparatus----- | 25 |
| 6 | Viewing Port Geometries----- | 27 |
| 7 | Combustion Chamber----- | 28 |
| 8 | Viewing Port----- | 29 |
| 9 | Glass Wool Particulate Trap----- | 31 |
| 10 | Vacuum System----- | 32 |
| 11 | Furnace----- | 34 |
| 12 | Hood Designs----- | 36 |
| 13 | Calibration Setup for PbO Reaction----- | 38 |
| 14 | Alignment Setup----- | 40a |
| 14a | Tube Tip Shapes----- | 44 |
| 15 | I ₂ Potential Curves----- | 52 |
| 16 | Vibrational Populations----- | 54 |
| 17 | Plot of Raw I ₂ Data and Predicted Transitions----- | 60 |
| 18 | Relative Intensity Profile----- | 60a |
| 19 | Proposed Hood Shape----- | 65 |
| 20 | Proposed Furnace----- | 67 |
| 21 | Gas Flushing Insert----- | 68 |
| 22 | View Port Heater----- | 68 |

List of Tables

| <u>Table</u> | | <u>Page</u> |
|--------------|--|-------------|
| I | Emission Lines of PbO----- | 2 |
| II | Flow Regimes----- | 20 |
| III | Flow Tube Performance----- | 47 |
| IV | Franck-Condon Factors for $I_2(B)_v \quad I_2(X)_v = 0$ ----- | 56 |
| V | Calculated $I_2(B) \quad I_2(X)$ Transitions----- | 59 |
| VI | PbO Flame Observations----- | 63 |

List of Symbols

| | |
|--------------|---|
| A | Area of flow tube |
| \AA | Angstrom (10^{-8} cm) |
| Ar | Argon |
| C | Conductance |
| cm | Centimeter |
| CETL | <u>C</u> hemical <u>E</u> lectronic <u>T</u> ransition <u>L</u> aser |
| D | Flow tube diameter |
| E/P | Ratio of field intensity to number density in a plasma |
| ev | Electron volt |
| HgO | Mercuric oxide |
| I | Iodine atom |
| I_2 | Iodine molecule |
| $I_2(x)$ | A form of spectroscopic notation signifying the ground electronic state of the I_2 molecule |
| $I_2(A)$ | The lowest energy electronic excited state of the same multiplicity as the ground state |
| $I_2(B)$ | The second lowest energy level |

List of Symbols (Cont'd)

| | |
|---------|---|
| j | Total angular momentum (spin and angular momentum) of an atomic electron |
| jj | A particular type of electronic coupling scheme in molecules; Hund's case C |
| J | Total angular momentum of an electronic state in a molecule |
| k | Boltzmann's constant |
| K_n | Knudsen's number |
| L | Recirculation zone length |
| M | Atomic mass number |
| mm | Millimeters |
| N_v | Population number of molecules in vibrational state v |
| N_2 | Nitrogen molecule |
| N_2^* | Activated nitrogen |
| N_2O | Nitrous oxide |
| NF_3 | Nitrogen trifluoride |
| O | Atomic oxygen |
| O_2 | Oxygen molecule |
| P | Pressure |

List of Symbols (Cont'd)

| | |
|-----------------|--|
| Pb | Lead |
| PbO | Lead oxide |
| Pb ₂ | Lead molecule |
| $g_{v',v''}$ | Franck-Condon Factor |
| Q | Throughput |
| r_e | Internuclear separation |
| R_e | Reynold's number |
| R_0 | Universal gas constant |
| Sp | Pumping Speed |
| T | Temperature |
| V | Velocity |
| V_e | Experimental velocity |
| V_{pf} | Velocity predicted by plug flow assumption |
| r | Atomic diameter |
| ϵ_v | Energy of an electron in cm^{-1} |
| ω_e | Oscillation frequency of molecule |
| χ_e | Anharmonicity constant of molecule |

List of Symbols (Cont'd)

| | |
|-------------------|--|
| λ | Mean free path |
| ρ | Density |
| η | Viscosity |
| Λ | Axial component of electron orbital angular momentum of molecule |
| Ω | Axial component of total electronic angular momentum |
| [] | Concentration of |
| α_{Σ} | $\Lambda = 0$, multiplicity of α |
| α_{Δ} | $\Lambda = 1$, multiplicity of α |
| α_{Γ} | $\Lambda = 2$, multiplicity of α |
| $\alpha(T)$ | Time dependent absorption coefficient |

Abstract

A gas flow tube was constructed to allow chemical reaction studies at pressures from 0.1 torr to 30 torr. The tube was designed to allow introduction of oxidants, diluents, or excited gases. A furnace was constructed to produce high temperature vapor in the combustion chamber of the flow tube.

The flow tube was characterized by its pumping speed, pressure, throughput, and evaluating Reynold's and Knudsen's numbers at pressures from 0.1 - 20 torr. Two experiments were conducted to verify the flow tube performance. Singlet molecular oxygen was produced in a microwave discharge and reacted with gaseous I_2 to yield chemiluminescence from the transition $I_2(B) \rightarrow I_2(X)$. The spectrum was recorded and the bandheads assigned to vibrational transitions predicted by theory. PbO was created by reacting vaporized lead with N_2O . The emissions were compared with literature.

A GAS FLOW TUBE
FOR SPECTROSCOPIC STUDIES

1. Introduction

Background

The military community has strong interest in the chemical electronic transition laser (CETL) (Ref 23:2), because of a number of very desirable features. These systems generate excited state molecules by chemical reaction; consequently, scale-up of such systems is not inhibited by the weight and volume of electrical power sources. Some molecules also exhibit electronic transitions in the near infrared, visible, and ultraviolet; thus, a laser utilizing these reactions could exhibit transmission properties in the atmosphere superior to current high power lasers such as the CO₂ (Ref 18).

The recent success of the so-called iodine laser (Ref 34) has demonstrated the viability of reactions involving the ¹Δ state of the O₂ molecule. This excited gas species exhibits a number of very desirable properties. First, the ¹ΔO₂ state has a radiative lifetime of about forty-five minutes, and is relatively immune to collisional deactivation with walls (Ref 2:2529). Second, oxygen in this state is readily produced in large quantities.

Another candidate laser pumping reaction is:



This reaction produces the electronically excited species, PbO* (Ref 42).

Hertzberg (Ref 29:564) and Shawhan et al. (Ref 43) list the following transitions of the PbO molecule.

TABLE I
Emission Lines of PbO

| <u>Transition</u> | <u>V_{00} (cm⁻¹)</u> | <u>λ (Å)^b</u> |
|-------------------|--|---|
| E ↔ x | 34755 ^a | 2936 |
| D ↔ x | 30103.2 ^a | 3322 |
| C ↔ x | 24762.0 ^a | 4156 |
| B ↔ x | 22173.4 ^a | 4510 |
| A ↔ x | 19728.3 ^a | 5069 |

^a All transitions shade toward red.

^b Emission lines reported.

All transitions are of desirable wavelengths for atmospheric propagation. Much previous work on PbO has been done

(Refs 6, 7, 8, 10, 33, 35, 36, 42), and the spectral structure of the system is well described. A fundamental problem arises, however, in that emission from the $\text{Pb} + \text{N}_2\text{O}$ reaction is reported as quite weak (Ref 33), although the reaction $\text{Pb} + \text{N}_2\text{O}$ is very efficient at producing ground state PbO . This raises the possibility that efficient chemiluminescence could be produced by collisions ground state PbO with excited molecular gas species with active nitrogen (Ref 33). One motivation for building a flow tube was to establish a system in which the investigation of the $\text{PbO} + \text{N}_2^*$ and $\text{PbO} + \text{O}_2^*$ could be performed. Many designs have been reported in the literature (Refs 1, 11, 13, 14, 20, 21, 22, 23, 24, 25, 26, 27, 46, 49, 52) and extensive work has been done on the PbO system in flow tubes (Refs 33, 36, 43). Consequently, it was decided to build a gas flow tube and modify it to allow chemiluminescence studies with gas phase reaction products, excited gases, or a combination of the two.

Objective

This thesis was intended to accomplish two goals. First, a gas flow tube would be built and modified from standard designs to allow the study of gas phase reactions in several ways. The flow tube design would be verified by reproducing the results of two widely studied reactive systems, $\text{O}_2(^1\Delta) + \text{I}_2$ and $\text{Pb} + \text{N}_2\text{O}$.

General Approach

A gas flow tube was used to react materials in the vapor phase with oxidants or excited gases. The resulting spectra were analyzed and the spectra compared with published data. The results were used to verify gas flow tube performance. The flow tube was characterized by Reynold's and Knudsen's numbers and system throughput. Some recommendations for further work are made.

II. Theory

Introduction

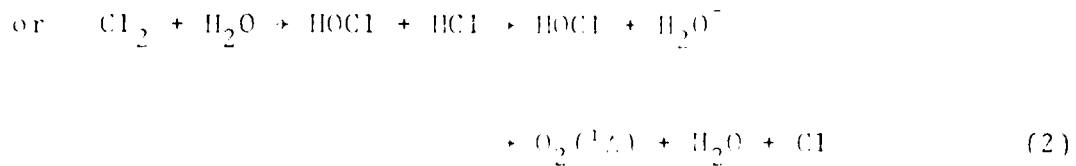
A brief account of the theoretical background pertinent to this thesis is presented in this chapter. First, a discussion of the genesis of this thesis is presented, with attention to Chemical Electronic Transition Inert Gas Discharge. Second, some general theory of gas flow reactors is presented. Last, the two reactions chosen to demonstrate the theory are presented, and the associated spectroscopy is discussed.

Background

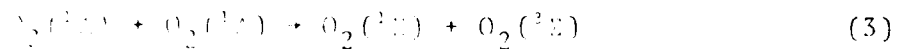
This thesis had its origin in a project at the Weapons Laboratory. In 1978, Melzer et al. (1) reported on the success of the Cl_1 laser. They utilized a gas flow reactor employing the following related reactions:

Singlet Molecular Production. Melzer employed a chemical production method. Gaseous Cl_2 is filled through a mixture of H_2O_2 and NaOH , and follows one of the reaction chains:





Part of the $\text{O}_2(^1\Delta)$ participates in an energy pooling reaction



Molecular iodine vapor is introduced, and dissociated as follows:



The chain reaction sequence is:

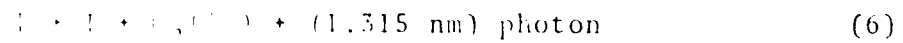


Figure 1 shows the energy levels for this system and for the I_2 molecule.

This system has proven to be very attractive for a CETL. Singlet O_2 has a radiative lifetime of 45 minutes (Ref 2:2529) and is resistant to collisional deactivation (Ref 2:2529).

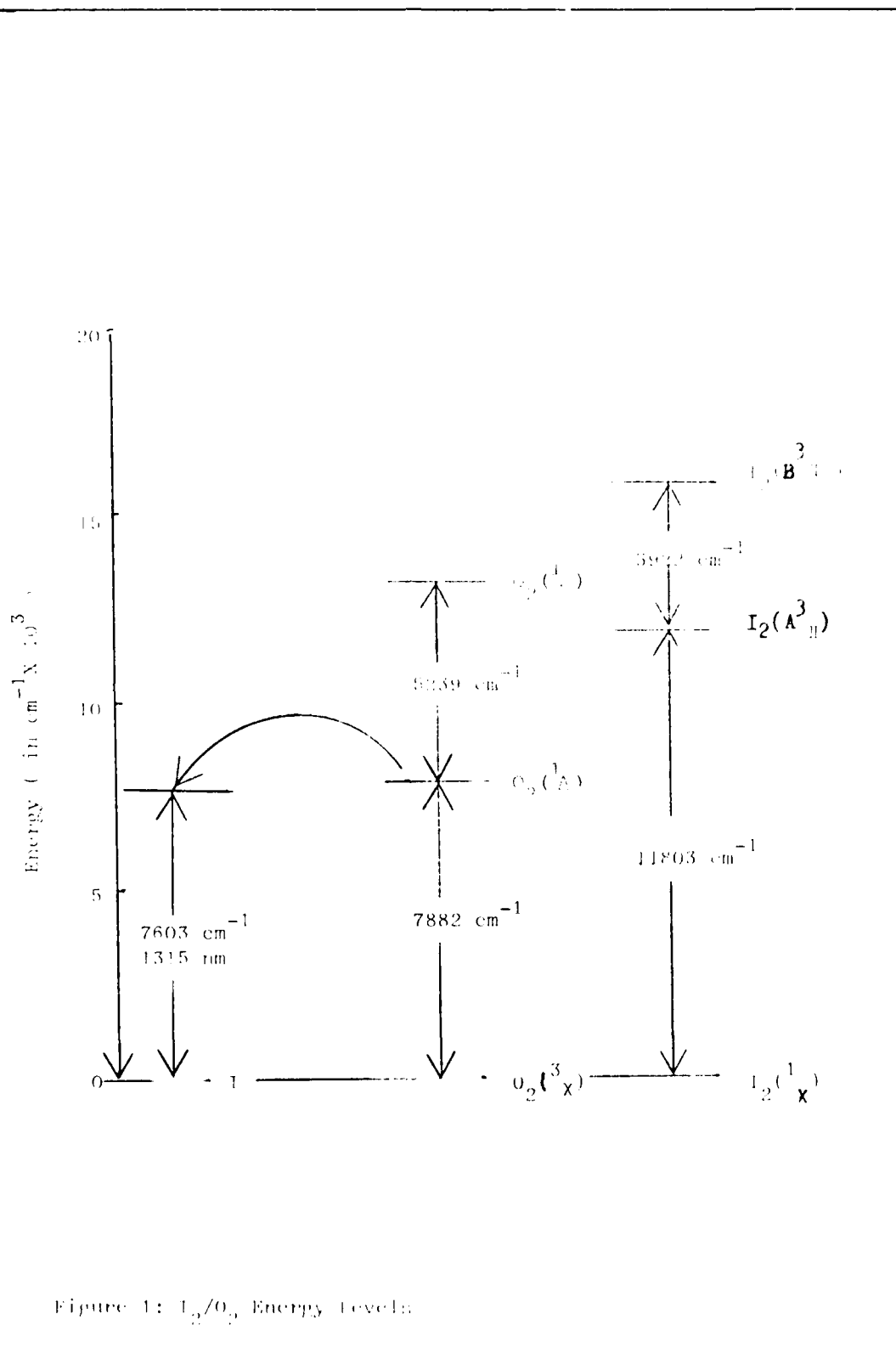


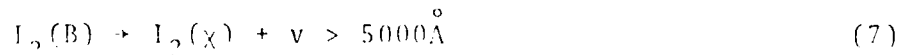
Figure 1: I_2/O_2 Energy Levels

The singlet states of molecular O_2 can be produced in large quantities via the chemical reaction shown in Eqs (1) and (2), and the O_2 effluent is benign. Iodine is recycled.

The success of this CETL has stimulated interest in a number of other chemical reactions as potential laser candidates, most of which can be studied effectively in a gas flow reactor.

Consequently, this thesis was designed to accomplish the task of building a gas flow reactor which could generate lasing candidates in a vapor state and react them with oxidizers or excited gases such as $O_2(^1\Delta)$ to produce vibronically excited species. The system chosen to demonstrate the flow tube capabilities was the I_2/O_2 system which exhibits yellow-green chemiluminescence. This reaction utilizes the same constituents as the I_2/O_2 laser, and there is a large amount of data in the literature for comparison. The capability to generate oxidant/high temperature vapor reactions was demonstrated by the $Pb + N_2O$ reaction. This system was chosen because most of its band structures lies in the visible region (thus simplifying the experimental setup and allowing a simpler measurement system), and because this system may be a candidate for a CETL.

I_2 Chemiluminescence. The chemiluminescence is generally agreed to result from emission from the $I_2(B)$ state (Refs 15, 16, 52). The reaction can be described by



Since analysis of the data is dependent on the emitting state and not on the excitation mechanism, no discussion will be presented in this section on the reaction mechanism. There is, however, a controversy about the $I_2(B)$ state formation and this will be discussed in Section VI.

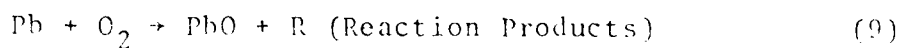
PbO

The PbO molecule is of interest because its spectra are extensively studied, the PbO molecule is amenable to excitation by a number of additives such as N_2^* and NF_3 (Ref 31:727), and because it is a candidate for a CETL. PbO formation from Pb and N_2O is exothermic, by 71.68 kcal/mol (Ref 31).

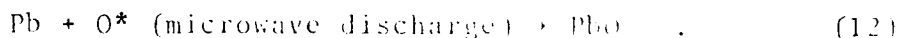
Reaction Methods. PbO emissions have been generated by a wide variety of reactions. Bloomenthal examined PbO spectra by using a lead arc in air (Ref 9:24). He also reports earlier efforts by Eder and Valenta who used lead chloride in an oxygen flame, and Grebe and Konen who used lead chloride in a carbon arc in air. Shawhan and Morgan (Ref 35:377) measured the A, B, and D systems and discovered the E system of PbO, using PbO heated in a furnace and irradiated by an ultraviolet source. More recently, Oldenberg, Dickerson and Zare studied the reaction



and Linton and Broida did a comprehensive study utilizing the reactions



and



The $\text{Pb} + \text{N}_2\text{O}$ reaction was chosen for the simplicity of production and the milder fouling problems reported by Linton and Broida (Ref 31).

Spectra. Herzberg reports the major electronic transitions listed in Table I.

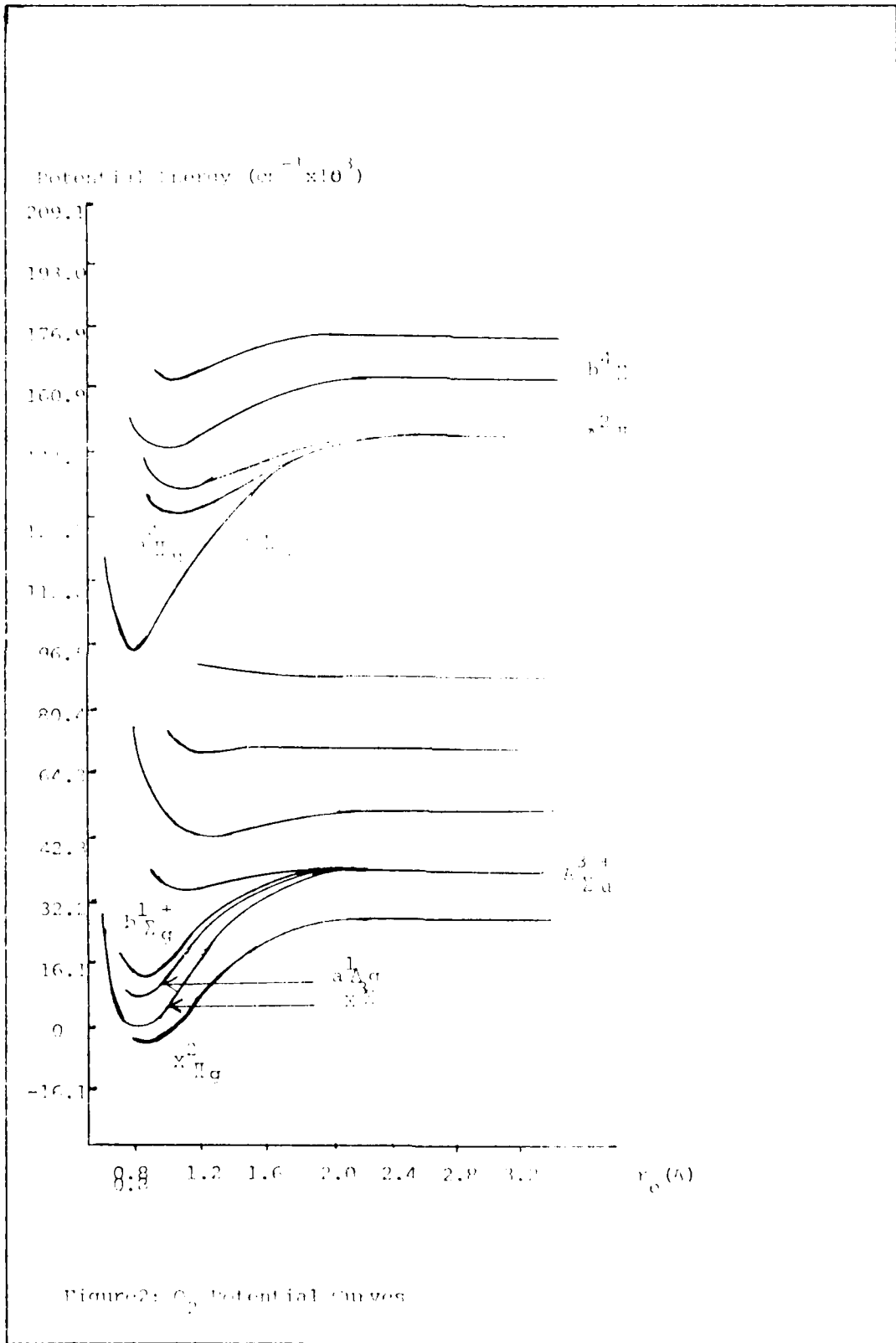
Numerous vibrational bands are reported; Linton and Broida report 33 bands for the $\text{A} \rightarrow \text{X}$ transition and 57 for the $\text{a} \rightarrow \text{X}$ transition (Ref 31). For a listing of PbO emission lines, see Appendix B. Linton and Broida show that $\text{Pb} + \text{N}_2\text{O}$ product spectra involve transitions from the $\text{a} \rightarrow \text{X}$, $\text{A} \rightarrow \text{X}$, $\text{B} \rightarrow \text{X}$, and $\text{C} \rightarrow \text{X}$ systems. No E or D

transitions are reported; this is possibly a limitation of their detection apparatus. They also report that, as pressure increased from 3.4 mm to 34 mm, the dominant emission changes from a pale blue flame (A → X, C → X systems) to a yellow-red flame (a → X, B → X systems).

Coupling. The electronic states of the Group IV chalconides can approach jj coupling for the heavy metals. For jj coupling, or more properly, Hund's case c, the coupling between L and S is stronger than the coupling between L or S and the internuclear axis (Ref 29:319). Thus, Λ and Σ are not good quantum numbers, and we consider that L and S couple to give J, with an axial component Ω. For this case, a number of general selection rules hold. The rule J = 0, ±1 holds, as does the symmetry rule + ↔ -, + ↔ +, - ↔ -. Since Ω is also a good quantum number, ΔΩ = 0, ±1; 0[±] ↔ 0[±], 0[±] ↔ 0[∓]. For the case of both states Ω = 0, ΔΩ = 0 is forbidden (i.e., no Q branch is allowed).

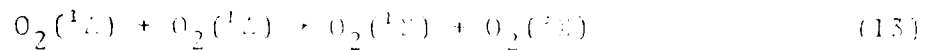
Singlet Molecular Oxygen. Excited oxygen was generated by passing the gas stream through a 2450 megahertz microwave discharge in a quartz plasma tube (Ref 48:287). Energy levels of the O₂ molecule are shown in Figure 2.

The major production mechanism for O₂(¹A) is direct electron impact excitation with ground state O₂ molecule by a 0.98 ev electron (Ref 18:246) with an energy of 7882.39 cm⁻¹ (Ref 29:540).

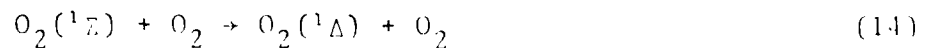


There are two major production mechanisms for the second metastable state, $O_2(^1\Sigma)$. The first is excitation by a 1.672 eV electron to the 13120.9 cm^{-1} energy level (Ref 29:540). This process is probably not competitive with the excitation to $O_2(^1\Delta)$, because the cross sections for excitation to $O_2(^1\Sigma)$ electron impact are approximately one order of magnitude lower than $O_2(^1\Delta)$ for the same electron energy (Ref 50:1482).

A second mechanism is the pooling reaction



Derwent and Thrush state that the concentrations of $O_2(^1\Sigma)$ and $O_2(^1\Delta)$ are $10^{-2} - 10^{-3}\%$, respectively (Ref 16:721). Although they do not specifically state how they arrive at these numbers, Thrush and Thomas report a method by which the concentrations are calculated from the emissions of $O_2(^1\Sigma)$ at $1.91 \mu\text{m}$ and $O_2(^1\Delta)$ at $1.27 \mu\text{m}$ (Ref 48:290). The $O_2(^1\Sigma)$ concentration is lower because of the lower cross section for excitation in the plasma, and because it is depopulated by



and



The second reaction shows a contrast to $O_2(^1\Delta)$ which is highly resistant to deactivation by wall collisions (Ref 3:1769).

An important by-product of the microwave reaction is atomic oxygen. In order to suppress O , a coating of H_2O_g is applied to the walls of the quartz tube. This coating catalyzes surface recombination of atomic oxygen (Ref 4:288).

Gas Flow Tubes

The flow patterns and velocities of a gas flow tube are of fundamental importance in determining the results of kinetic experiments. Two of the criteria for flow tube design arose from an examination of flow phenomena.

Recirculation and Flow Restrictions. The first design criterion was the requirement to minimize flow restrictions and sudden expansions or contractions of the tube. Flow restrictions decrease the conductance of the system; conductance being a measure of the efficiency with which gas can be pumped through the tube. An example of a restriction would be a series of successively smaller tube diameters towards the vacuum pumps.

A sudden expansion or contraction of the tube diameter can generate a recirculation zone such as the one shown in Figure 3. Recirculation was examined by Pennucci (Ref 38:11) as part of the problem of suddenly expanded gas flows.

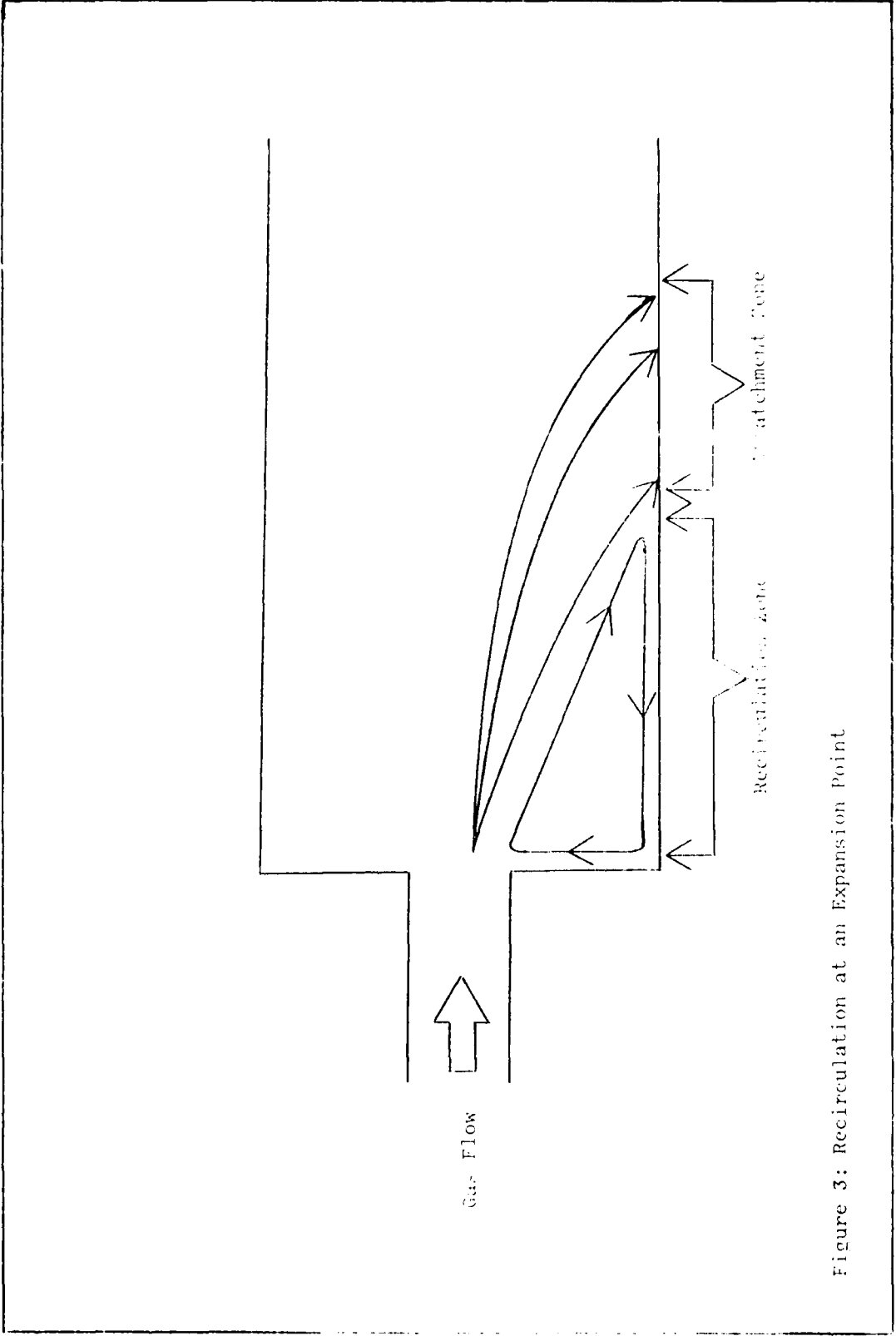


Figure 3: Recirculation at an Expansion Point

Referring to Figure 3, a schematic depiction is given of the vortex phenomena known as recirculation. Gas molecules in the recirculation zone L may remain for some time before reattaching to the flow in the attachment zone. This phenomenon is significant when attempts are made to create a flame, since in an improperly designed chamber, the reaction may occur in the recirculation zone rather than the viewing area downstream (see Chapter V).

Velocity Profiles and Flow Characterization. The second design criterion was that the system operate in the laminar flow regime. A more rigorous definition is given below, but in general terms a flow may be characterized as turbulent, laminar, or molecular. The importance of laminar flow may be understood as follows: picking a simple example, the rate of consumption of reactant, A, in a chemical reaction can be expressed as

$$\frac{d[A]}{dt} = k[A]^n \quad (16)$$

where $[A]$ is the concentration of A, k is the reaction rate coefficient, and n is the power dependency of the reaction on the concentration of A. To evaluate $\frac{d[A]}{dt}$ in a flow tube experiment, we may write

$$\frac{d[A]}{dt} = \frac{d[A]}{dx} \frac{dx}{dt} \quad (17)$$

where $\frac{d[A]}{dx}$ is the change in $[A]$ as a function of some distance scale, usually longitudinal in the flow tube. We can then interpret $\frac{dx}{dt}$ as the gas velocity, and evaluate $\frac{d[A]}{dx}$ in terms of some observable such as the intensity of a given emission.

This approach requires that $\frac{dx}{dt}$ be well defined. A common assumption is that of plug flow, which assumes the linear velocity to be everywhere uniform. This assumption holds true for the turbulent flow regime, but breaks down badly for the laminar case (Ref 50). The turbulent case presents problems, though, in that the gas number densities may exhibit local deviations from isotropy (turbulent cells), with the effects on the gas kinetics being difficult to predict.

Wolf showed that the velocity can be defined for laminar flow in a flow tube (Ref 50). For the molecular flow case, however, the assumption that the time rate of change of concentration is proportional to the linear velocity since there may not be a well defined linear velocity. Thus the second criterion was to confirm that the system exhibited laminar flow. The following sections describe the flow regimes, the equations for evaluating flow tube performance, and present a limited discussion of parameters useful in calculating flow rates.

Flow Regimes. A gas flow tube may be characterized in part by the conditions under which gas flow takes place. Generally speaking, flow can be turbulent, laminar, or molecular. Figure 4 depicts velocity profiles for the turbulent and laminar cases.

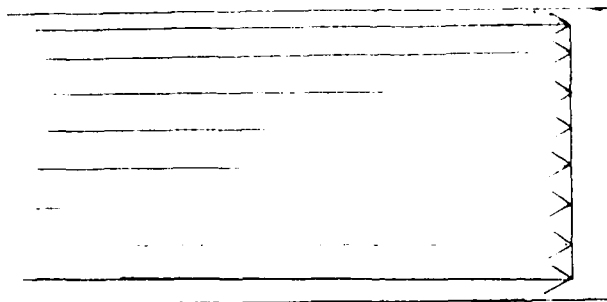
Viscous Flow. A volume at pressure P_1 is connected to a second volume at pressure P_2 through an aperture of size A_1 with $P_2 < P_1$. If P_1 is such that the mean free path of a gas molecule, λ , is small compared to the dimensions of A , the flow is viscous (Ref 40:62). The velocity of the gas can be increased by lowering P_2 until the ratio P_2/P_1 reaches a critical value; the speed of sound for that gas (Ref 40:67). At this point, further reductions of P_2 will not increase the flow rate. Thus, we see that merely adding more pumps for a given cavity is pointless if a flow tube is operating in the viscous regime, once the critical P_2/P_1 ratio has been reached.

When operating in the viscous region, a gas flow tube may exhibit turbulent or laminar flow. The dividing line between turbulent and laminar is determined by the tube's Reynold's number, Re , where

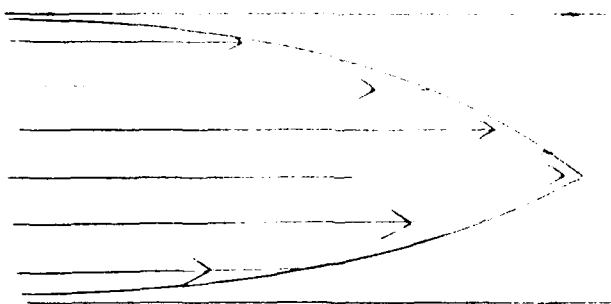
$$Re = \rho v D / \eta \quad (\text{Ref 40:61}) \quad (18)$$

and ρ is the gas density, v the linear gas stream velocity,

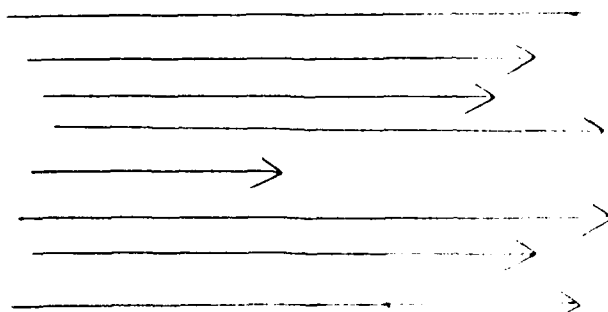
Plug Flow Assumption Profile



Laminar Flow Profile



Turbulent Flow Profile



Length of Arrow Indicate Relative Velocities Within Profile
Figure 4: Velocity Profiles Under the Turbulent, Laminar, and Plug Flow Regimes.

the viscosity, and D the diameter of the tube. Generally, an Re greater than 2100 indicates completely turbulent flow, and Re less than 1100 indicates completely laminar flow.

Molecular Flow. The dividing lines between viscous, intermediate, and molecular flow are determined by Knudsen's number, defined as the ratio D/λ , where D is the flow tube diameter and λ the mean free path. Table II summarizes the regime boundaries, after Roth (Ref 40:61).

TABLE II
Flow Regimes

| | <u>Flow Regime</u> | <u>Re, D/</u> |
|------------|--------------------|---|
| Viscous | Turbulent | $Re > 2100$ |
| | Laminar | $Q > 200D$ (air) $D/\lambda > 110$, $Re < 1100$ |
| | | $Q < 100D$ (air) |
| Transition | Intermediate | $1 < D/\lambda < 110$ |
| Rarified | Molecular | $D/\lambda < 1$ |

Throughput Q. The throughput is a measure of the quantity of gas moving through a pipe per unit time. Roth defines the throughput Q as $PV (\pi D^2/4)$ where the units are as previously defined. In general, the flow in the viscous regime will be turbulent if Q is greater than 200D, and laminar if Q is less than 100D.

An empirical formula for Q in air is

$$Q_{\text{air}} = 9.06 \times 10^{-2} \text{ Re}D, \text{ in torr-liter/sec} \quad (19)$$

(Ref 40:61)

Knudsen's Number. Knudsen's number (K_n) is used to delineate the boundaries between viscous, intermediate, and molecular flow. K_n is defined by

$$K_n = D/\lambda \quad , \quad (\text{Ref 3:67}) \quad (20)$$

where D = diameter of the flow tube, and λ is the mean free path (Ref 42:67). A general expression for the mean free path of a gas in a flow tube is given by Roth

$$\lambda = kT/\sqrt{2} \pi \epsilon^2 P \quad (\text{Ref 40:37}) \quad (21)$$

where k = Boltzmann constant, 1.3805×10^{-16} erg/°K, T is the gas temperature in °K, P is the gas pressure, and ϵ is

the molecular diameter. As an example, an empirical formula for λ of air at ambient temperature is

$$\lambda = 5 \times 10^{-5} / P \quad (\text{Ref 40:37}) \quad (22)$$

Conductance. When steady state flow is achieved in a flow tube, the number densities of two adjacent sections of pipe are related by Eq (23),

$$N = C(n_1 - n_2) \quad (\text{Ref 40:63}) \quad (23)$$

Here, N is the number of molecules crossing a cross section of the pipe, n_1 and n_2 represent the number densities in the respective sections, and C is the conductance (Ref 40:63). The conductance for a pipe of dimension D , length L , and operating at pressure P is given by Eq (24),

$$C = (P\pi D^4) / (128 \eta L) \quad (\text{Ref 40:74}) \quad (24)$$

For air at 20° C, Eq (24) reduces to

$$C_{\text{air}} = 182 (D^4 / L) P \quad (\text{Ref 40:74}) \quad (25)$$

The pumping speed, S , in a chamber connected by conductance C to a pump having speed S_p is given by Eq (26),

$$1/S = 1/S_p + 1/C \quad (\text{Ref 40:66}) \quad (26)$$

This can be rewritten as

$$S/S_p = (C/S_p)/[1 + (C/S_p)] \quad (27)$$

Equation (27) shows that increasing the pump size S_p does not increase S if the conductance is the limiting factor (Ref 40:66).

Plug Flow. In his master's thesis, Wolf examined a traditional assumption employed in gas flow work; the plug flow assumption (Ref 50). After the Wolf thesis, the difference between plug flow, laminar, and turbulent flow can be visualized as in Figure 3. Wolf determined deviations from the plug flow assumption on the order of 1.6 - 1.8 for the ratio V_e/V_{pf} , where V_e is the experimental centerline velocity and V_{pf} is the predicted or plug flow velocity (Ref 53:55). This phenomenon is very important in interpreting gas kinetic data, or any experiment in which radiative lifetimes or downstream intensities are measured.

III. Experimental Apparatus

Introduction

A brief description of the apparatus is given in this chapter. In building the apparatus, two criteria were considered paramount. First, the tube was to be designed to allow high flow rates with dynamic pressures as low as 0.1 - 0.2 torr. To achieve this condition, special attention was paid to the vacuum system and to system layout. Second, previous papers report severe problems in system fouling, especially in the Pb + N₂O reaction (Ref 33). A number of schemes were evaluated for dealing with this problem and for solving the problem of maintaining a clear viewport.

Flow Tube

The flow tube (see Figure 5) was assembled from component parts manufactured by Alloy Products. The tube was constructed of three inch inner diameter stainless steel pipe. The ends of each section have an O-ring groove to provide a vacuum tight seal. The connections between sections are made with quick flanges.

Input Section. The input section serves three purposes in this apparatus. Excited gases were introduced through a gasketed end plate on the transition section in the I₂/O₂

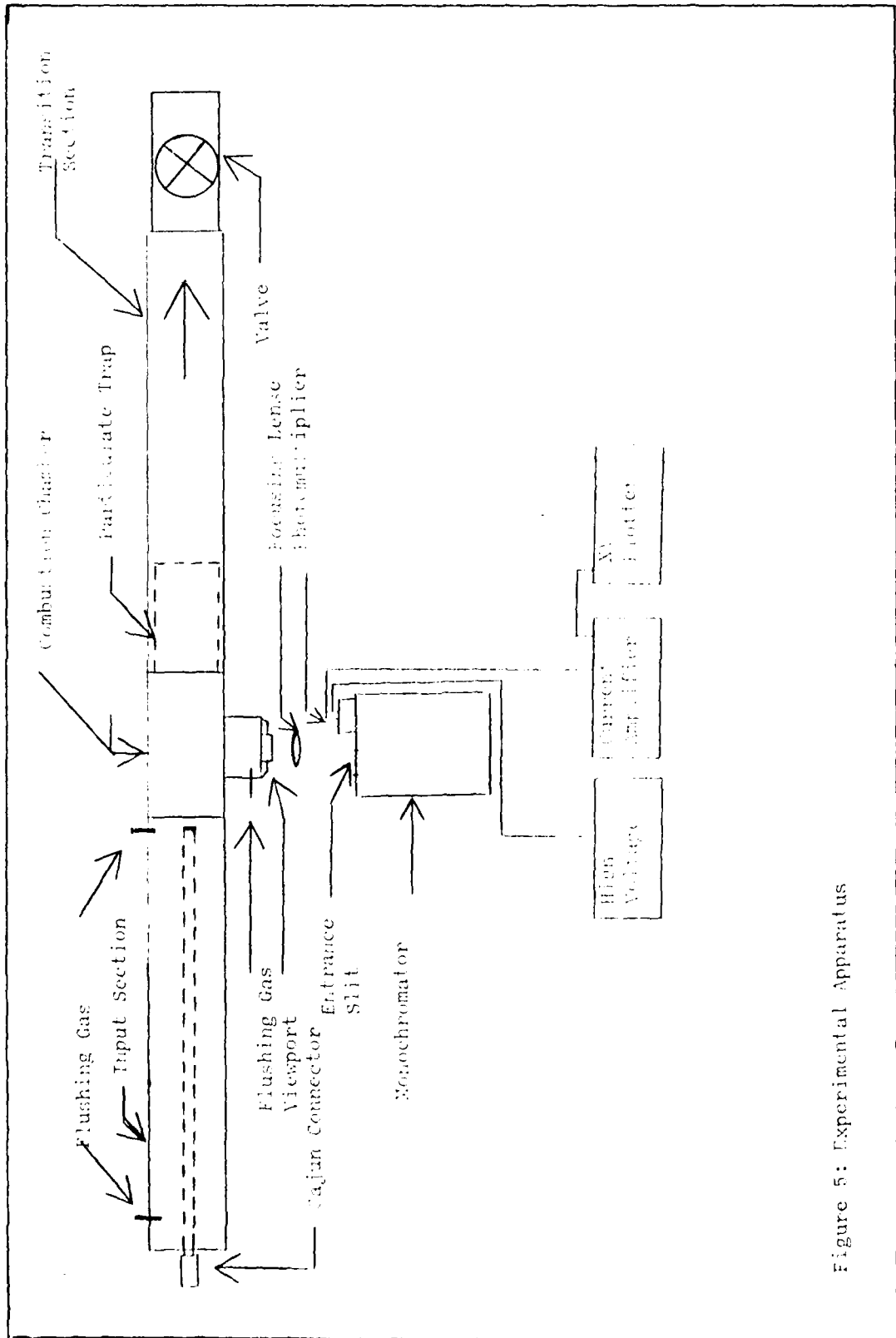


Figure 5: Experimental Apparatus

chemiluminescence experiment. During the PbO experiment, a viewing arm was placed at the front of the input section and inlets provided for flushing gases (see Figure 6). Finally, quenching gases can be introduced upstream of the reaction chamber.

Combustion Chamber. The combustion chamber in which the reaction being studied took place was a commercial "T" made by Alloy Products. An additional arm was added as shown in Figure 7, and for the viewing port an end plate (see Figure 8) had a 2.5 inch hole counter-sunk in the face, and a centered, 0.75 inch hole was bored through. A 0.25 inch thick glass plate was seated over an O ring into the hole, and the vacuum pull allowed to seal it. This design facilitated rapid cleaning of deposits.

Previous investigators have experienced severe fouling problems in oxidizer/metal vapor reactions (Ref 33:399). Two approaches were tried to solve this problem. The viewing port on the combustion chamber (Figure 7) has a 0.0625 inch inner diameter tube inlet through the wall in front of the viewport. Gas could be introduced in front of the viewport to create a flowing gas barrier to the reaction product.

The second approach was to place a 24 inch section of pipe upstream of or normal to the combustion chamber (Figure 6). The extension had gas inlets identical to the

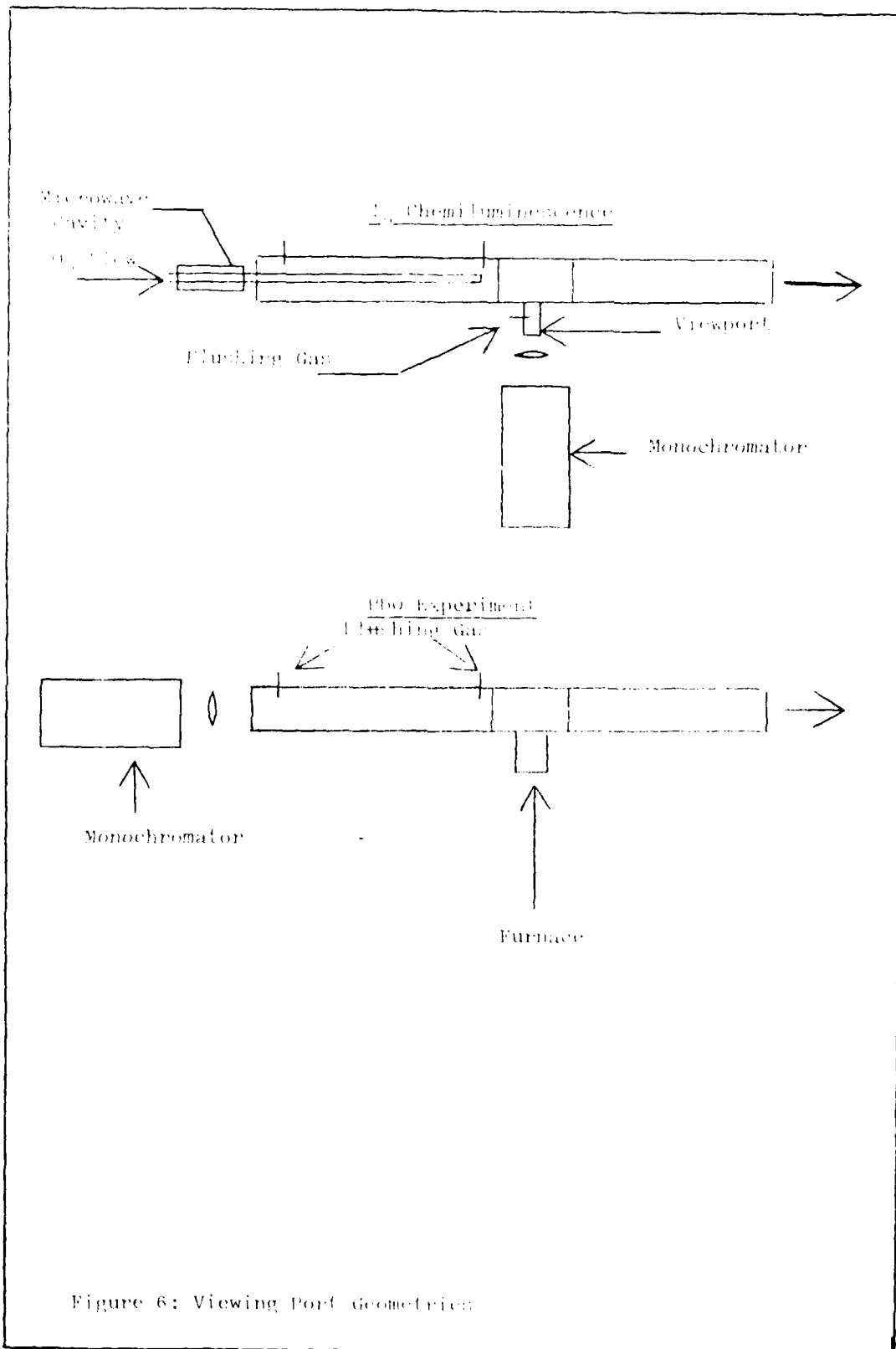


Figure 6: Viewing Port Geometries

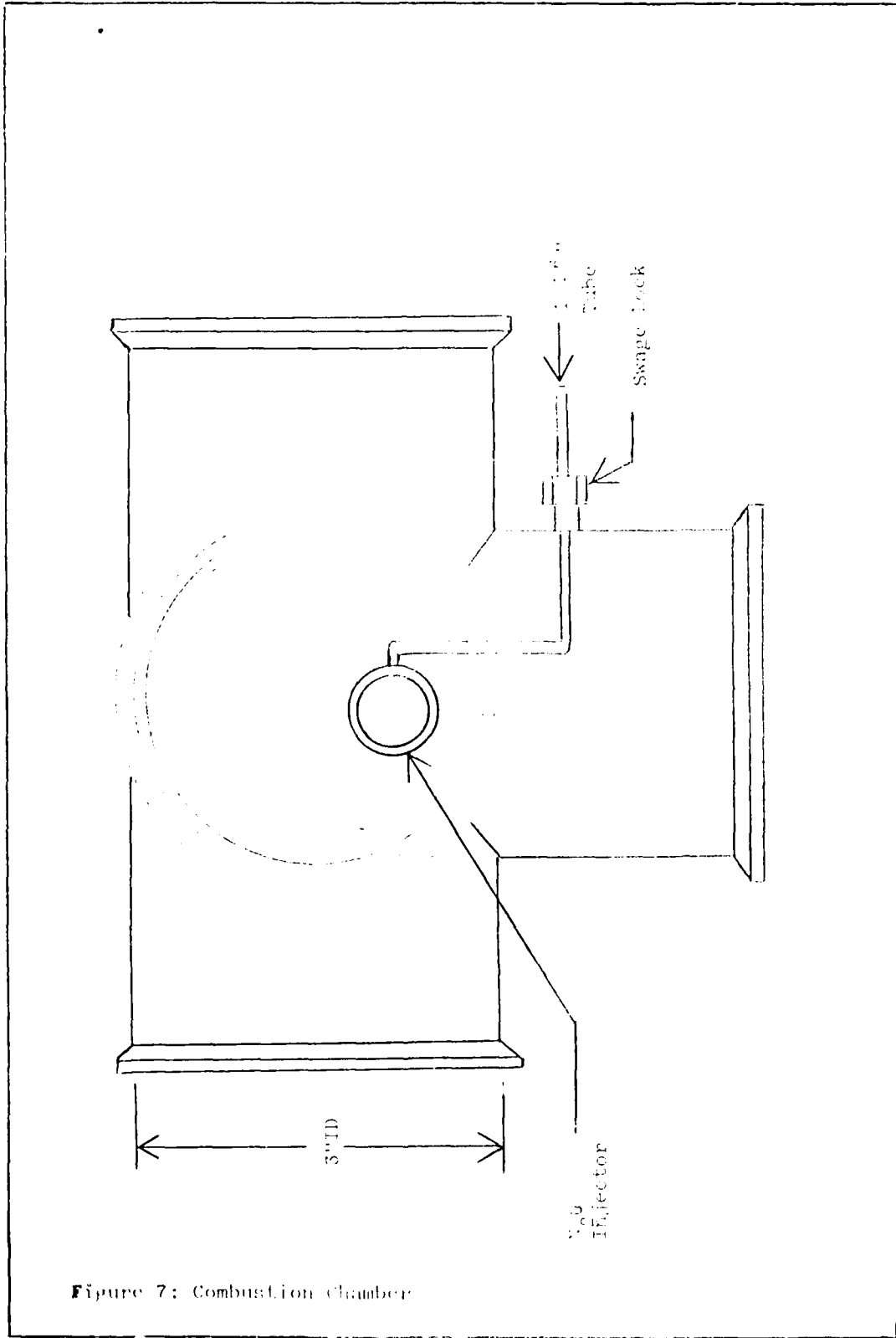


Figure 7: Combustion Chamber

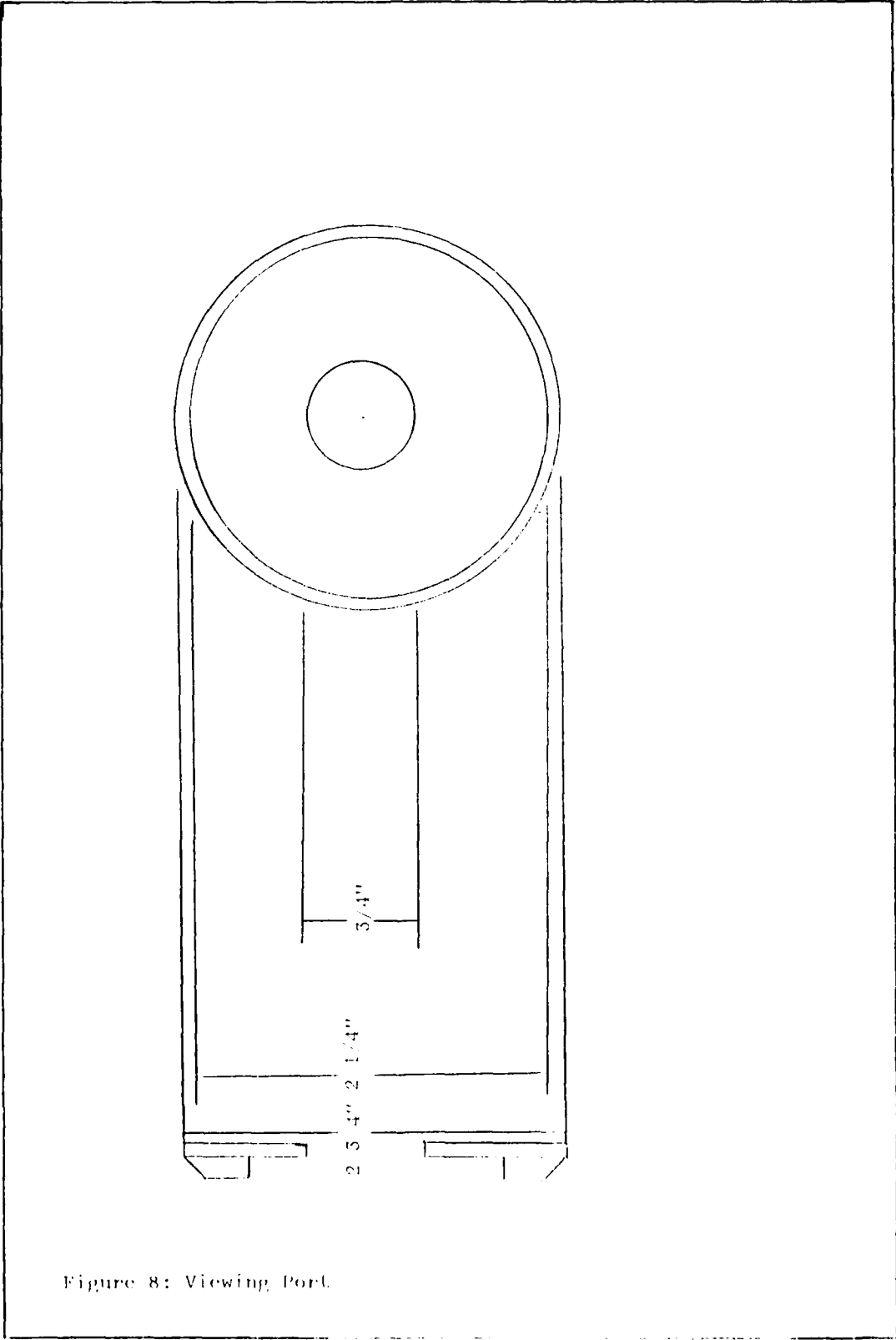


Figure 8: Viewing Port.

one on the combustion chamber, and flushing gases were introduced ahead of the viewport.

An additional experiment was devised to reduce fouling downstream of the combustion chamber (Figure 9). A 3.0 outer diameter stainless steel pipe section had a screen wire welded to the bottom, and this pipe was inserted into the downstream leg of the combustion chamber. This pipe was then filled with glass wool and the effect of the device on pumping efficiency and tube fouling was evaluated.

Oxidizers were introduced into the combustion chamber through an injector as shown in Figure 7. This shape was chosen over a number of widely used shapes (Ref 25:722) because it gave a brighter and more uniform flame.

Transition Section. A 2.0 foot section was incorporated downstream of the combustion chamber. Gas kinetic studies could then be performed by replacing the stainless steel tube with a glass tube.

Pumping Section. Immediately following the transition is an adaptor which goes from the 3.0 inch stainless steel to a 1.75 inch inner diameter pipe. The adaptor has a port for measuring pressures (Figure 10).

Provisions were made to install a cold trap immediately downstream of the adaptor to remove atomic iodine before it reached the vacuum pumps (Figure 10). The cold trap

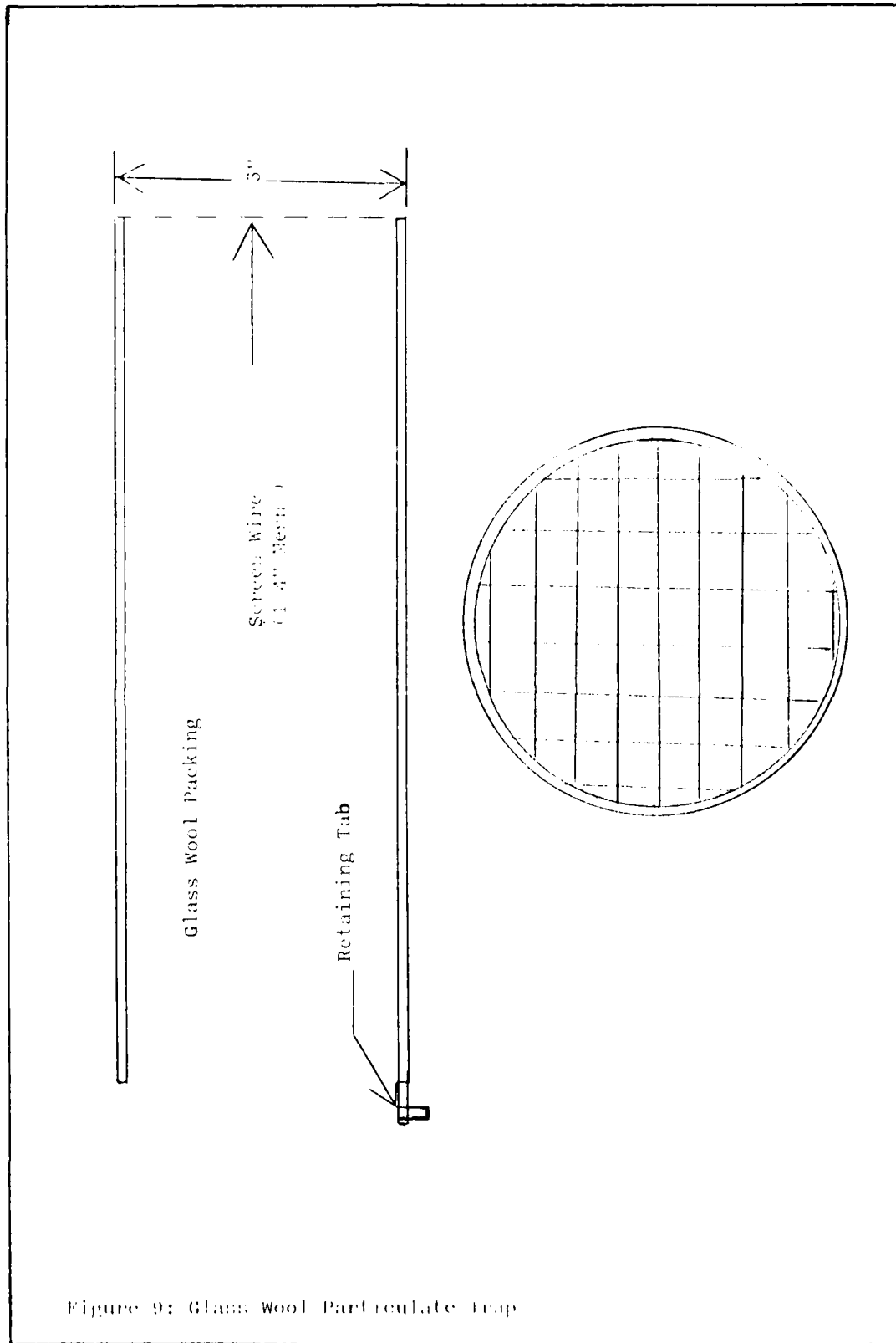


Figure 9: Glass Wool Particulate Trap

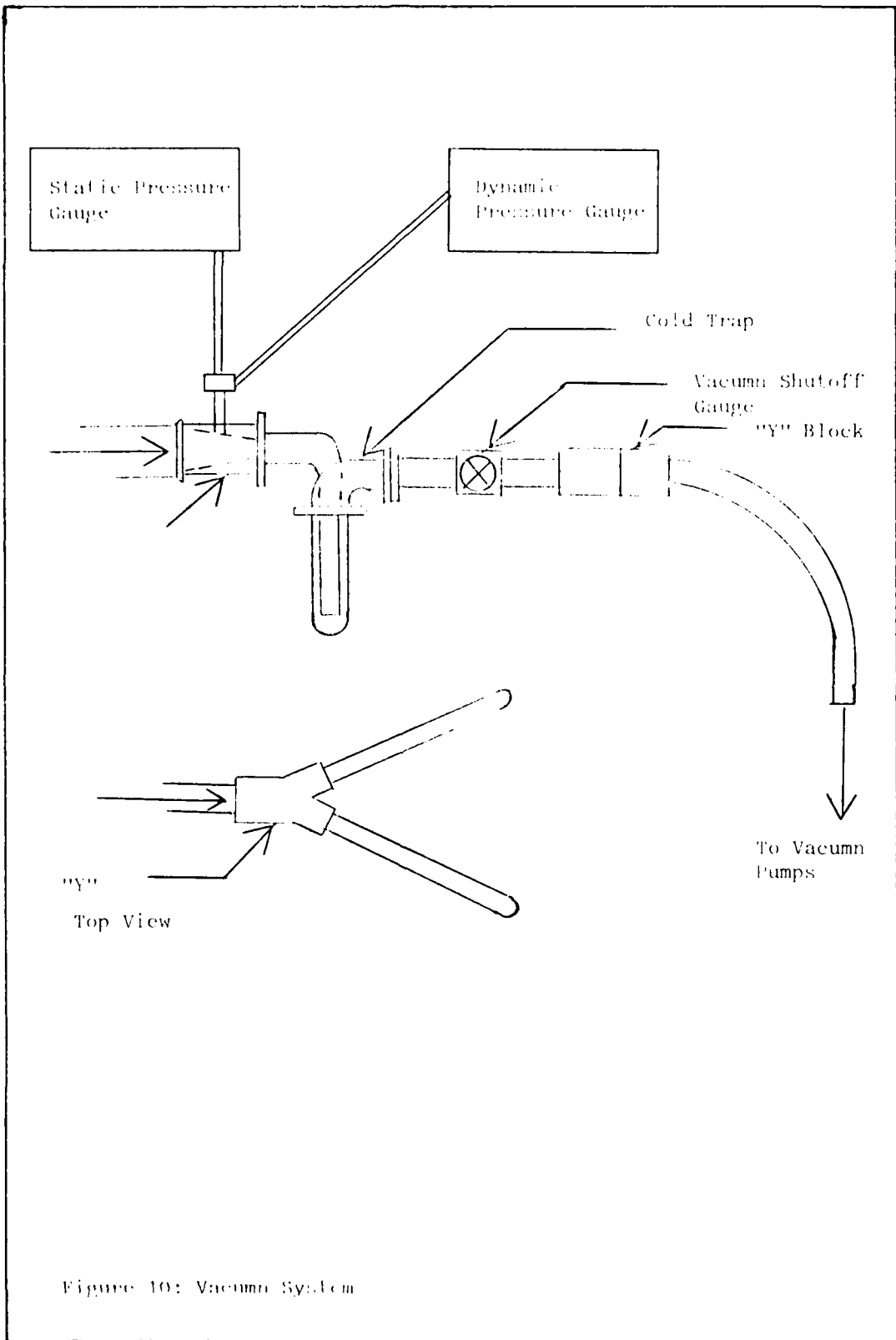


Figure 10: Vacuum System

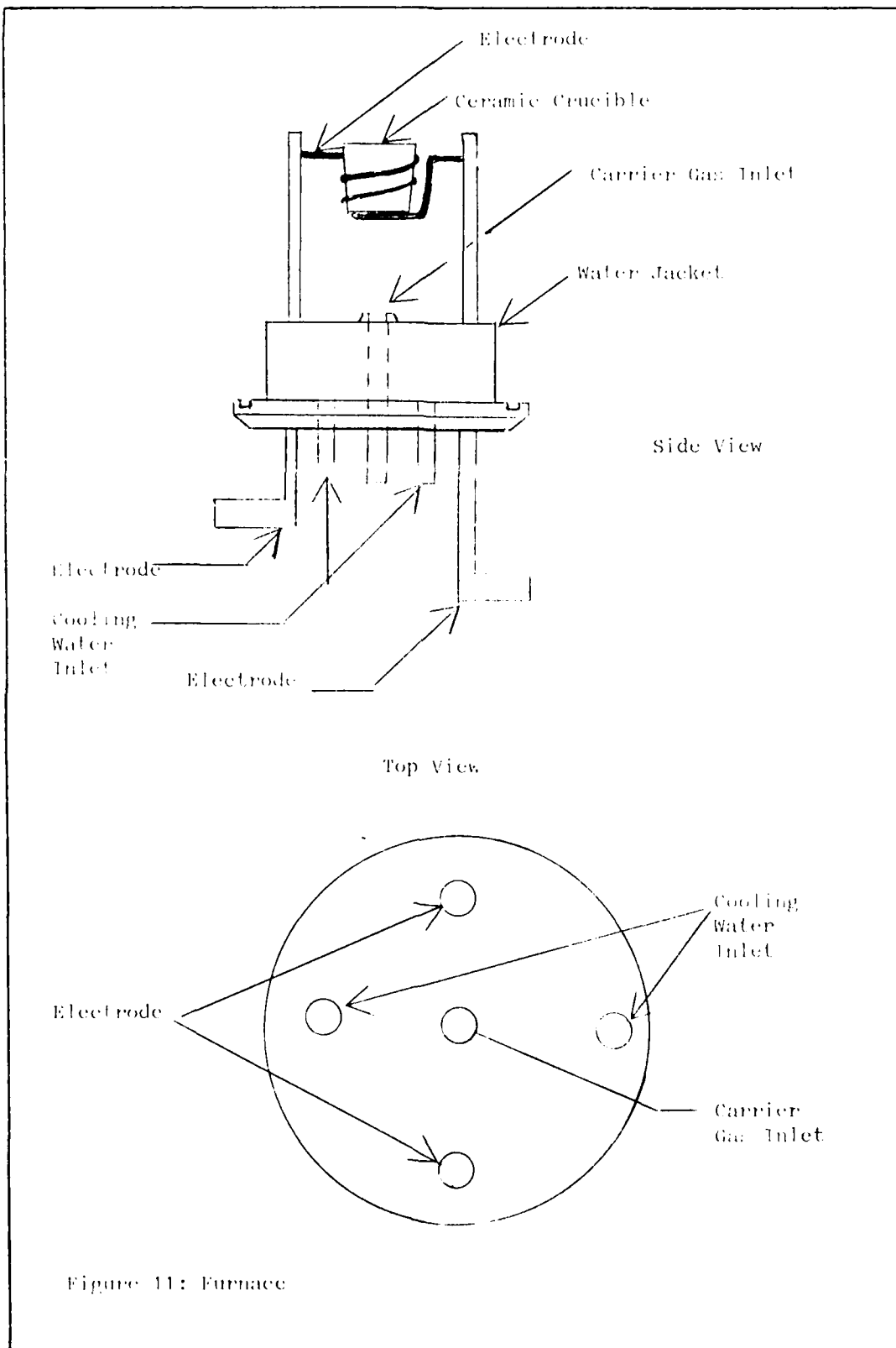
was cooled with a dichloromethane-dry ice slush (approximately -60° F). Downstream of the adaptor or cold trap, an 8.0 inch long, 1.75 inch inner diameter pipe connected to a Consolidated Vacuum 1.5 inch ball valve (Figure 10). Another 1.75 inch pipe downstream of the ball valve connected to a "Y" as shown in Figure 10. The downstream legs of the "Y" connect to 1.375 inch inner diameter pipes which curve on a 24 inch radius to the vacuum pumps. The connections to the pumps are made with vacuum hose to minimize transmitted vibration. The pumps are 17.0 CFM Welch floor pumps.

Vapor Generation

Iodine. Iodine vapor was produced by passing AR gas stream over I_2 crystals in a 1/4" inner glass tube. The vapor pressure of iodine is approximately 1 mm at room temperature. This pressure was adequate to give useable concentrations.

Lead. With a melting point of 327.3° C (Ref 28), Pb requires a high temperature furnace of some sort. An electric furnace was constructed, as in Figure 11, along the lines suggested by Dr. S. Davis (Ref 13).

Power was provided from a 28 volt, 600 amp Rapid Electric Company Model S-528 D.C. generator. Current was fed through No. 4 cables to electrodes cooled by a water jacket.



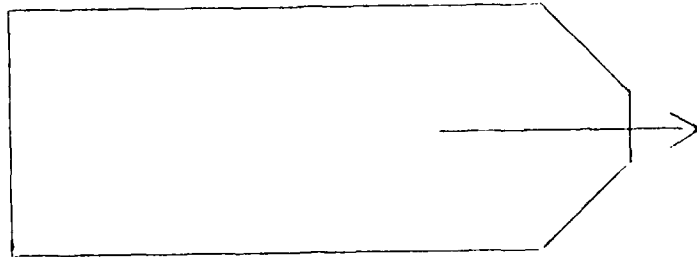
The current heated a crucible which contained reagent grade lead shot. The resulting vapor was entrained in an Ar carrier which took it to the viewing region. A number of schemes were tried for baffling the glow of the furnace while shaping the flow of entrained lead for maximum brightness. A few hood designs are shown in Figure 12. Excess heat was eliminated by water cooling the electrodes and wrapping copper water cooling pipe around the outside of the furnace and viewing chamber.

Measurement System

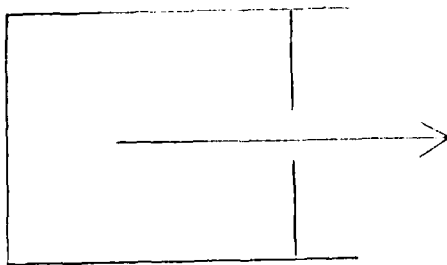
The spectrograph was a Jarrel-Ash 0.5 m scanning monochromator, with a diffraction grating ruled to 1180 grooves/mm, and blazed with a reciprocal dispersion of $16 \text{ \AA}/\text{mm}$ in first order. The resolution was 0.2 \AA in first order. The light was focused on the entrance slit of the monochromator with an 8.7 cm focal length lens for iodine, and a 15.0 cm focal length lens for lead (see Figure 6). Plots of relative intensity vs. wavelength were recorded.

The signal for the I_2/O_2 experiment was received by a 1P21 photomultiplier biased at 1000 volts by a Keithley 244 high voltage source. The 1P21 has an anode sensitivity of $1.2 \times 10^5 \text{ A/W}$ at 4000 \AA . For the PbO reaction, a more sensitive RCA 7265 photomultiplier tube with an anode sensitivity of $3.0 \times 10^6 \text{ A/W}$ was substituted. Appendix D shows typical response curves for these tubes. The signal

a. Simple Conical



b. Endplate With Hole



c. Chimney

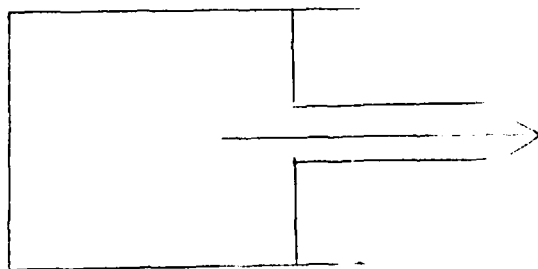


Figure 12: Hood Design.

was amplified by a Keithley 427 current amplifier and recorded on a Houston Instruments Omnigraphic 2000 X-Y plotter.

Microwave. The microwave source was a Kiva MPG-3 driving an Evenson-Broida cavity cooled with gaseous N_2 . The gas feed tube was 14 mm diameter quartz, which was coated inside by blowing O_2 over Hg and passing the mixture through the cavity at 100 watts forward power. This produced a yellow-brown HgO coating whose purpose was to eliminate atomic oxygen in the excited products. The gas tube was introduced through a connector (manufactured by Cajon, Inc.) into the flow tube, which allowed the position of the tube relative to the flame to be varied. The plasma was ignited with a Tesla coil.

Ancillary Equipment

Calibration Lamps. Calibration was performed with an Hg lab standard from Ultraviolet Products. The 5460.7, 5769.6, and 5790.7 Å lines were selected for calibration marks. For the I_2/O_2 experiment, a separate calibration run was performed using the Hg calibration lamp. During the PbO reaction, the high sensitivity of the 7265 photomultiplier tube precluded direct observation of the Hg lamp without inducing unacceptable noise. Therefore, the setup shown in Figure 13 was devised.

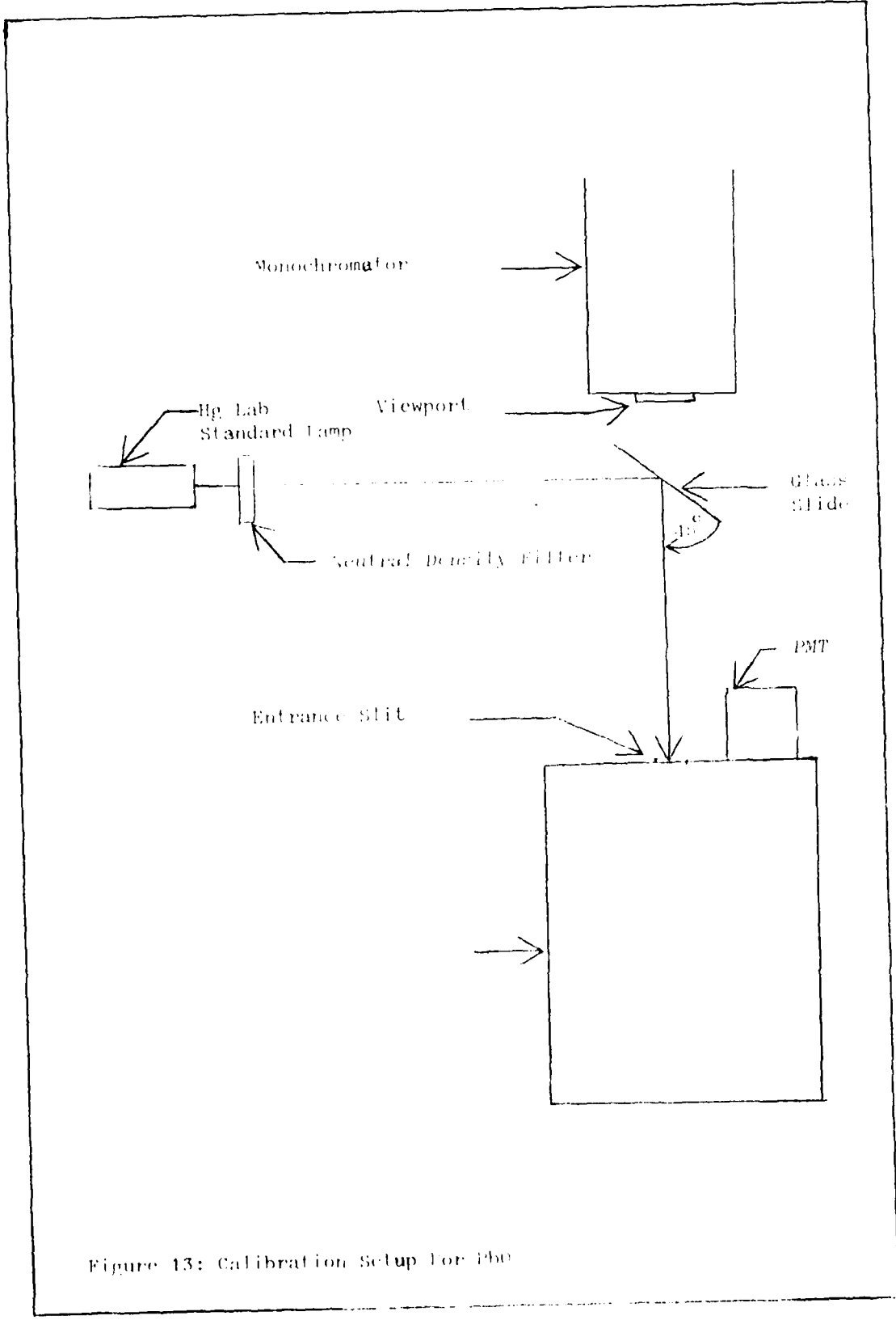


Figure 13: Calibration Setup For Pb0

Gas Manifold and Feed. All gas connections were made with 1/4" swage-lock Hoke valves and 3/16" inner diameter stainless steel pipe. The N_2O was routed through a manifold so that, if necessary, it could be diluted with inert gases.

Pressure. A "T" was installed on the adaptor pressure monitoring port to allow dynamic and static pressure sensors to be attached. Static pressure was measured with a Hastings 0 - 1 torr gauge and served as a vacuum integrity check. Dynamic pressure was measured with a Baratron MKS Type 77 pressure gauge. The use of this gauge allowed precise measurement of dynamic pressures as low as 0.01 torr.

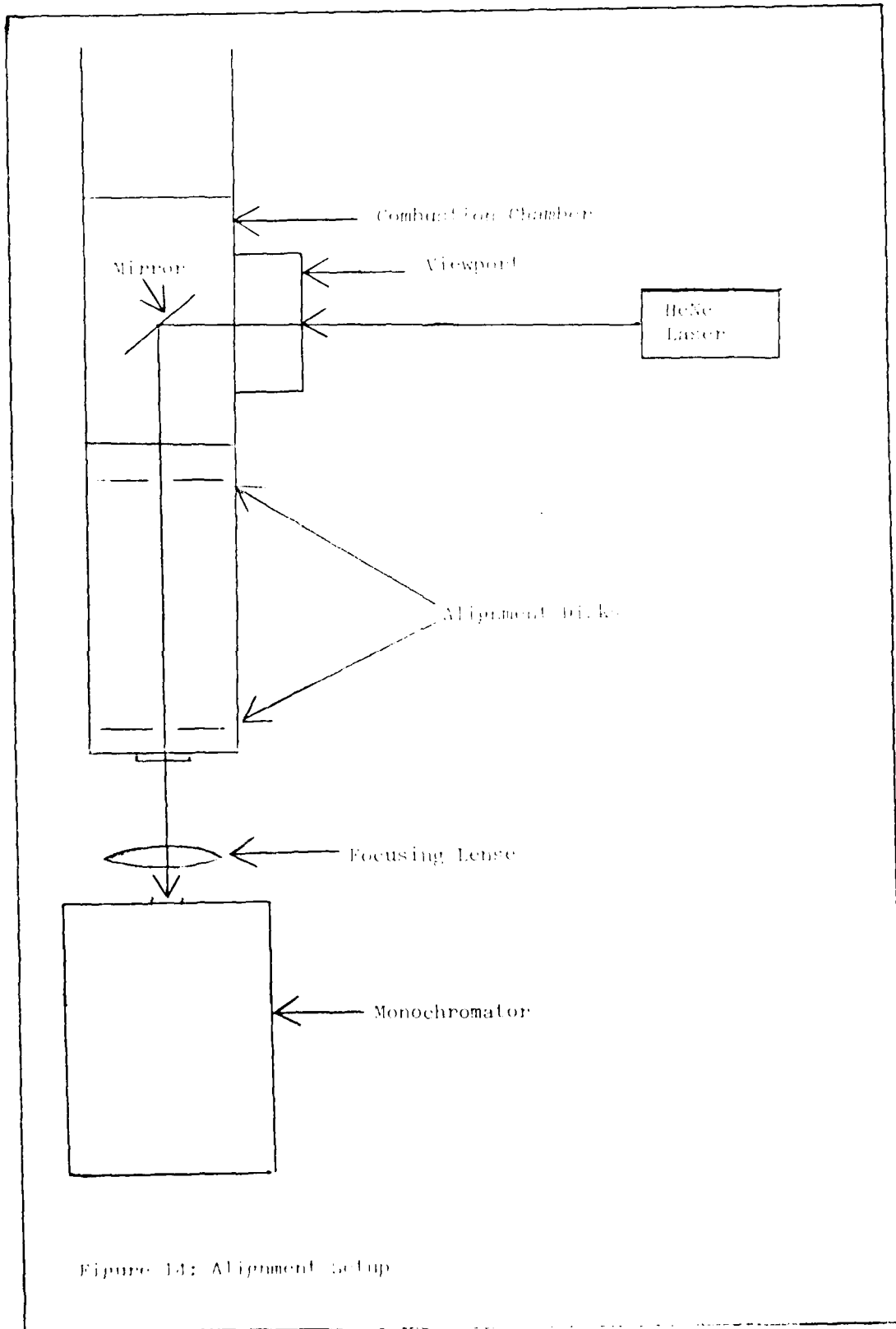
IV. Experimental Procedure

Introduction

It is appropriate to treat the experimental procedure in four sections. The first, starting and shut-down for a flow tube of this type, is covered as a list in Appendix A. The second section deals with alignment and calibration of the flow tube and spectrograph, while the third deals with the requirements of data collection in the F_2/O_2 and Pb/N_2O experiments. The last section discusses some particular safety hazards encountered.

Alignment and Calibration

Alignment. The tube and spectrograph were aligned using a Spectra-Physics 142P 2 mW HeNe laser. A mirror was mounted in the combustion chamber at a 45° angle to the tube axis, and the beam was introduced through the orthogonal viewing port. The exiting beam entered the entrance slit as shown in Figure 14, and the spectrograph was adjusted for a maximum signal at $6328\overset{\circ}{\text{Å}}$. Since the sensitivity of the 1P21 photomultiplier at $6328\overset{\circ}{\text{Å}}$ is well below the peak response, it was felt the maximizing the signal in this fashion would guarantee good response between 4000 and $6000\overset{\circ}{\text{Å}}$.



The Jarrel-Ash monochrometer was calibrated according to the manufacturer's manual using an Ultraviolet Products Hg lab standard lamp. The uncertainty in wavelength is given as $\pm 0.2\overset{\circ}{\text{Å}}$ by the manufacturer (Ref 30).

The large error induced by the gear lash in the monochrometer required a different calibration technique for the PbO experiment. The PbO molecule has a very large number of transitions in the visible, and assignment of these transitions would be very difficult with an uncertainty much greater than $1\overset{\circ}{\text{Å}}$.

The solution was to insert a glass slide between the viewport and the lens. The slide was placed at a 45° angle to the axis of propagation, resulting in a 3% transmission loss of the signal (see Figure 12). When the monochrometer approached a calibration peak of the Hg lamp, the shutter would be tripped and a cal mark placed directly on the spectrum. With this method, the uncertainty is estimated as $1\overset{\circ}{\text{Å}}$ (from data plots).

During the I_2/O_2 experiment, calibration was performed by returning the spectrograph to the starting point after a spectrum had been taken and re-running with the Hg lamp in front of the slit. At pre-selected wavelengths, the lamp would be uncovered and the calibration wavelength recorded. Gear lash on the monochromator was estimated to add $\pm 3\overset{\circ}{\text{Å}}$ error to this procedure.

The width of the calibration spike at a scanning speed of $500\overset{\circ}{\text{Å}}/\text{min}$ and slit width of 0.6 mm was approximately 1Å FWHM, so the total uncertainty in a transition wavelength was $\pm 4.2\overset{\circ}{\text{Å}}$ as given by Eq (28).

$$\begin{aligned} \Delta\lambda &= \text{calibration} & + & \Delta\lambda \text{ gear} \\ & \text{monochromator} & & \text{lash} \\ & + \text{peak width} & = & 0.2\overset{\circ}{\text{Å}} + 3\overset{\circ}{\text{Å}} + 1.0\overset{\circ}{\text{Å}} \\ & & & = 4.2\overset{\circ}{\text{Å}} \quad (28) \end{aligned}$$

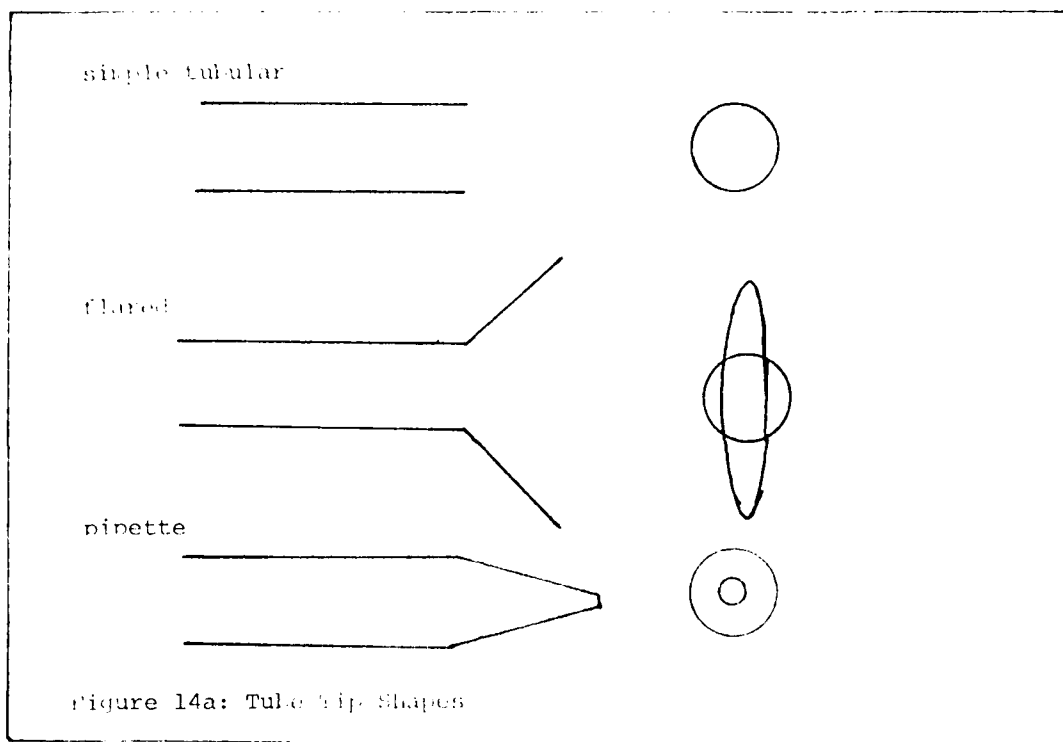
Alignment

An RCA 7265 photomultiplier was used for the Pbo experiment. Since the 7265 is very sensitive to system noise, the following procedures were used. First, two-prong adaptors were used to float all electronics, except for the x-y plotter which was grounded to the building water system. This prevented ground loops. Next, the x-y plotter was zeroed with no input, and the 7265 biased at 100 volts. With all light sources off or covered, the gain on the current amplifier was turned up until it went to 1/4 full scale, then the dark current bias turned on to bring it to 0. The voltage was turned up in increments of 100 volts and plotted against the dark current until the tube response went non-linear, then the voltage was decreased by 100 volts.

Data Collection

Microwave. Experimentation with the microwave was in two areas. First a variety of ignition methods, power settings, and gas flow rates were attempted to optimize the flame. The best results were obtained with an O_2 pressure of 0.5 - 1.5 torr with a forward power of 100 watts and with reflected power minimized. The best ignition method was found to be an arc generated by a high voltage Tesla coil applied just upstream of the cavity. Pressures of less than 0.5 torr O_2 generated an extremely hot plasma, with attendant cooling difficulties, while it proved very difficult to sustain a plasma with O_2 pressures over 1.5 torr. The second area of experimentation involved optimizing the position and shape of the tube tip for the region where the $O_2(^1\Delta)$ left the glass tube and entered the combustion chamber. Tip shapes evaluated included a simple tubular tip, a fan shaped tip, and one with a reduced exit diameter. Tip positions were varied from 0.5 inches to 6.0 inches from the vapor column. The optimum flame was generated with a simple tubular tip 0.5 inches from the vapor train. Figure 14 shows some of the tube tips tried.

Iodine Production. I_2 was produced by entraining I_2 vapor in a pipette with an Ar diluent. Although other groups have tried methods such as heating or photo-excitation (Ref 53), ample I_2 was obtained in this experiment



by the vapor pressure at room temperature. The gas was then introduced to the $O_2(^1\Delta)$ stream with a pipette.

Flame Tuning. The flame was trimmed by varying the $O_2(^1\Delta)$ and Ar pressure. An optimum flame occurred at 1.5 mm O_2 and 0.5 mm of Ar. The intensity was relatively independent of cavity geometries.

Pb + N_2O . Pb was heated in an electric furnace (see Figure 10). The resulting vapor was entrained in Ar at pressures of 0.5 - 20.0 torr. N_2O was introduced in the burner ring described earlier at pressures of 0.5 to 20.0 torr. The resulting flame was observed at right angles to the flowing gas and from an on-axis point upstream of the

combustion chamber. Power input to the heating coil to vaporize the lead varied from 200 - 1100 watts of DC power. The intensity of the flame was a strong function of the power input. The brightest flame occurred at the highest power input.

The Pb atoms were then entrained in Ar. The mixture was passed through the center of the N₂O ring and N₂O was introduced at various pressures. The N₂O was also mixed with an Ar diluent to observe the effect.

It was discovered in the course of the PbO experiment that power levels higher than 600 watts severely degraded the lifetime of the heating coils. The optimum value of 540 watts was chosen for the data runs.

Safety

PbO is listed as a class 3 inhalant hazard (Ref 42), which means that it is dangerous in milligram quantities, and so precautions were taken to avoid inhalation. Filter masks were worn whenever the combustion chamber was opened. The work area was vacuumed after every chamber opening and the contaminated areas were sponged. The flow tube was kept under vacuum between runs.

V. Results and Discussion

This section discusses the gas flow tube performance, the I_2/O_2 chemiluminescence experiment, and the results of the $Pb + N_2O$ experiment. Extensive tabulations of data from literature are recorded in Appendix B for the PbO molecule.

Gas Flow Tube Performance

This section discusses the flow regimes of the flow tube and the results of experiments undertaken to improve flame intensity and reduce system fouling from the various reactions. Table III summarizes the flow tube performance.

The Reynolds number was evaluated using Eq (18), where the density ρ is given by Eq (29)

$$\rho = \frac{M \text{ (atomic weight/mole)} P \text{ (gas pressure in mm)}}{R_0 T (^{\circ}K)} \quad (29)$$

(Ref 40:61)

The velocity was determined using the empirical formula in Eq (30)

$$V = \frac{Q P \text{ (atmospheric pressure in mm)}}{60 P \text{ (gas pressure in mm)} \Lambda \text{ (area for tube)}} \quad (30)$$

(Ref 53:31)

TABLE III
Flow Tube Performance^a

| <u>FLOW RATE</u> (cm ³ /min) | <u>TUBE PRESSURE (Torr)</u> | <u>Re</u> | <u>λ (cm)</u> | <u>Kn</u> | <u>COMMENT</u> |
|--|-----------------------------|-----------|----------------------|-----------|----------------|
| 0 ^b | 0.1 | | 50x10 ⁻³ | 152 | Laminar Flow |
| 900 | 2.0 | 16.70 | 2.5x10 ⁻³ | 3048 | Laminar Flow |
| 1700 | 3.0 | 31.55 | | | |
| 2450 | 4.0 | 45.57 | | | |
| 2950 | 5.0 | 54.75 | | | |
| 3900 | 6.0 | 70.55 | | | |
| 4500 | 7.0 | 83.52 | | | |
| 5250 | 8.0 | 97.45 | | | |
| 5750 | 9.0 | 106.73 | | | |
| 6500 | 10.0 | 120.65 | 3x10 ⁻⁴ | 15240 | Laminar Flow |
| 6900 | 11.0 | 128.07 | | | |
| 7200 | 12.0 | 133.64 | | | |
| 7600 | 13.0 | 141.06 | | | |
| 7950 | 14.0 | 147.56 | | | |
| 8250 | 15.0 | 153.13 | | | |
| 8500 | 16.0 | 157.77 | | | |
| 8900 | 17.0 | 165.19 | | | |
| 9100 | 18.0 | 168.91 | | | |
| 9500 | 19.0 | 176.33 | | | |
| 10000 | 20.0 | 185.61 | 2.5x10 ⁻⁴ | 30480 | Laminar Flow |

^a All data were taken at 760 torr (30.16 in Hg) ambient, and 19° C (292° K)

^b Meter would not record flow rate.

The mean free path, λ , was calculated using Eq (22). Knudsen's number was calculated using Eq (2). The results listed in Table III demonstrate that the design goals were achieved. Pressures as low as 0.1 torr were recorded and flow was laminar in all velocity regions.

If gas kinetics are done in this system, the velocity calculated from Eq (30) should be multiplied by a correction factor ranging from 1.6 to 1.8 to account for deviations from the plug flow assumption. Wolf's thesis (Ref 53:47) addresses this issue at length. Section VI contains recommendations for an assessment of this correction factor.

System Features

Various ideas for improving flow tube system performance were evaluated. This section will assess their effectiveness.

Hood Designs. Figure 12 shows the various hood designs which were inserted above the furnace to shape the vapor flow. Hood design 12a was effective aerodynamically, in that no evidence of recirculation (PbO or Pb₂ plating) was seen outside the chimney. Its major defect was that high Ar pressures were needed to get the Pb vapor up to the orifice and keep the N₂O out. These pressures cooled the Pb vapor and caused condensation inside the hood unless very high voltages (16 - 18 volts) were applied, which reduced

the life of the heater wires. Additionally, the high currents used created a large background glow which tended to obscure the signal from 6000 to 7000 $\overset{\circ}{\text{A}}$.

Figure 12b depicts the second hood design, which attempted to shorten the distance the Pb vapor had to travel to reach the viewing region. The 1/2" diameter hole was designed to cut down the background glow. The poor aerodynamics of this design created recirculation zones at points 1 and 2, as witnessed by the large lead deposits at 1 and PbO deposits at 2. It proved impossible to get the flame into the viewing region with this design.

Figure 12c depicts the successful design. It was recognized that the chimney would generate a recirculation zone, but by placing the tip of the chimney just below the viewing region, the reaction was forced to proceed in front of the view port. At low pressures, the flame extended well above the chimney.

Anti-Fouling. Two approaches were taken to solve the fouling problem. The first was to isolate the viewport by placing it well upstream of the reaction chamber. This approach eventually worked. The second approach was to use flushing gases to create an air window in front of the viewing port, as shown in Figure 6. This approach worked well when the viewing port was well away from the reaction, but failed when the port was placed very close to the

reaction, as in Figure 6 where the view is from 90° to the tube's axis. An attempt to blow gas directly onto the viewport (Figure 7) entrained Pb_2 and PbO and resulted in a completely opaque coating within 30 seconds. The tactic of locating the monochromator away from the combustion chamber did cut down the signal intensity, so further refinement is required.

I_2 Experiment

It was decided to verify I_2 chemiluminescence in two ways. First, bandhead positions for transitions from the $I_2(B)$ state to ground would be calculated from published spectroscopic constants and compared to the data obtained in this thesis. Second, the relative intensity profile, corrected for photomultiplier response and absorption due to plating of the view port, would be compared to published data.

Correlations With Predicted Bandheads. Certain assumptions were made in calculating the bandhead positions. Figure 15 shows a potential curve for the $I_2(B,A,X)$ states of the iodine molecule.

Predicting the inter-electronic transitions for these required a knowledge of which vibrational states were populated in $I_2(B)$. Derwent and Thrush showed that $I_2(B)$ at room temperature displayed the behavior shown in

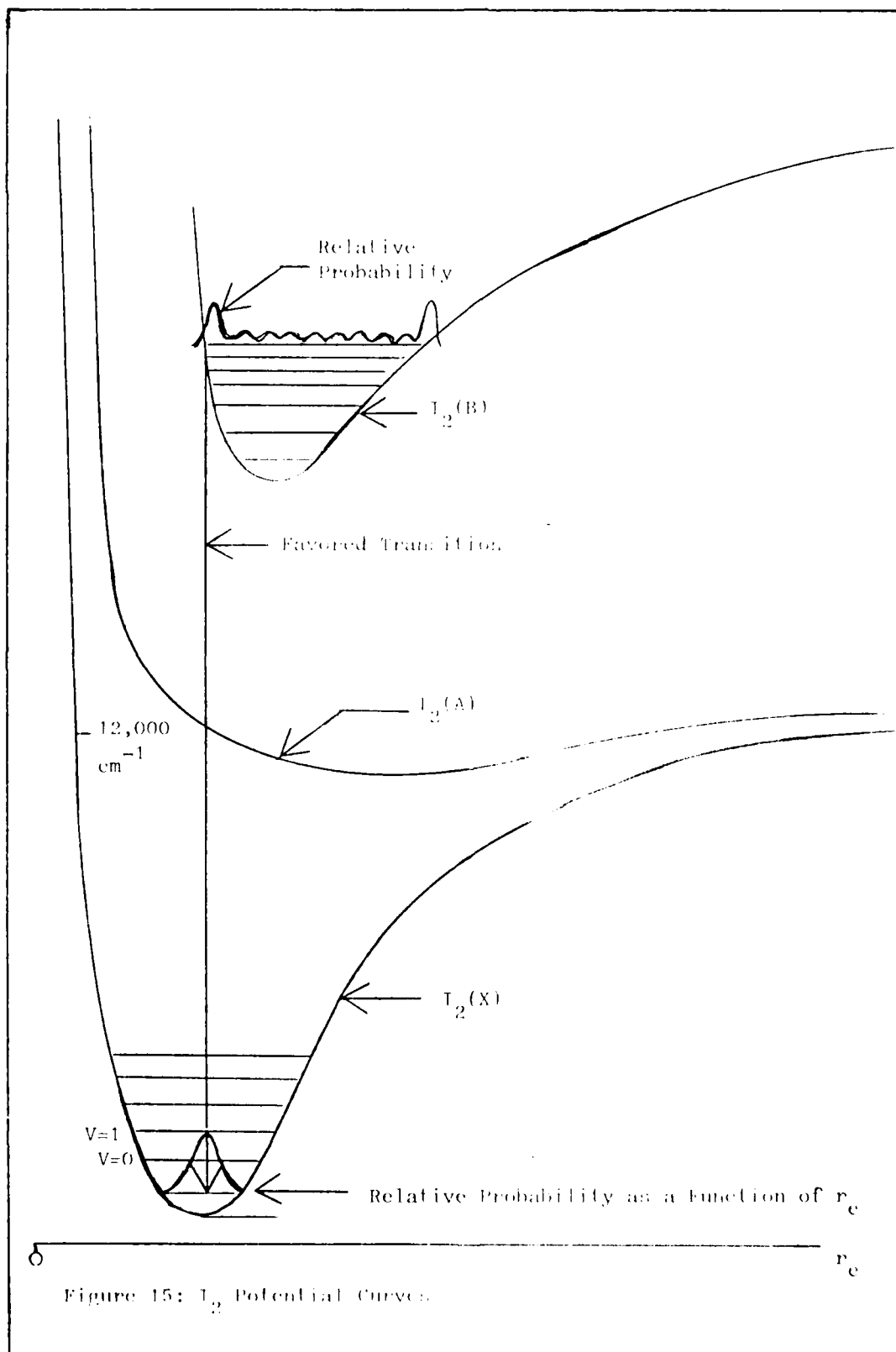


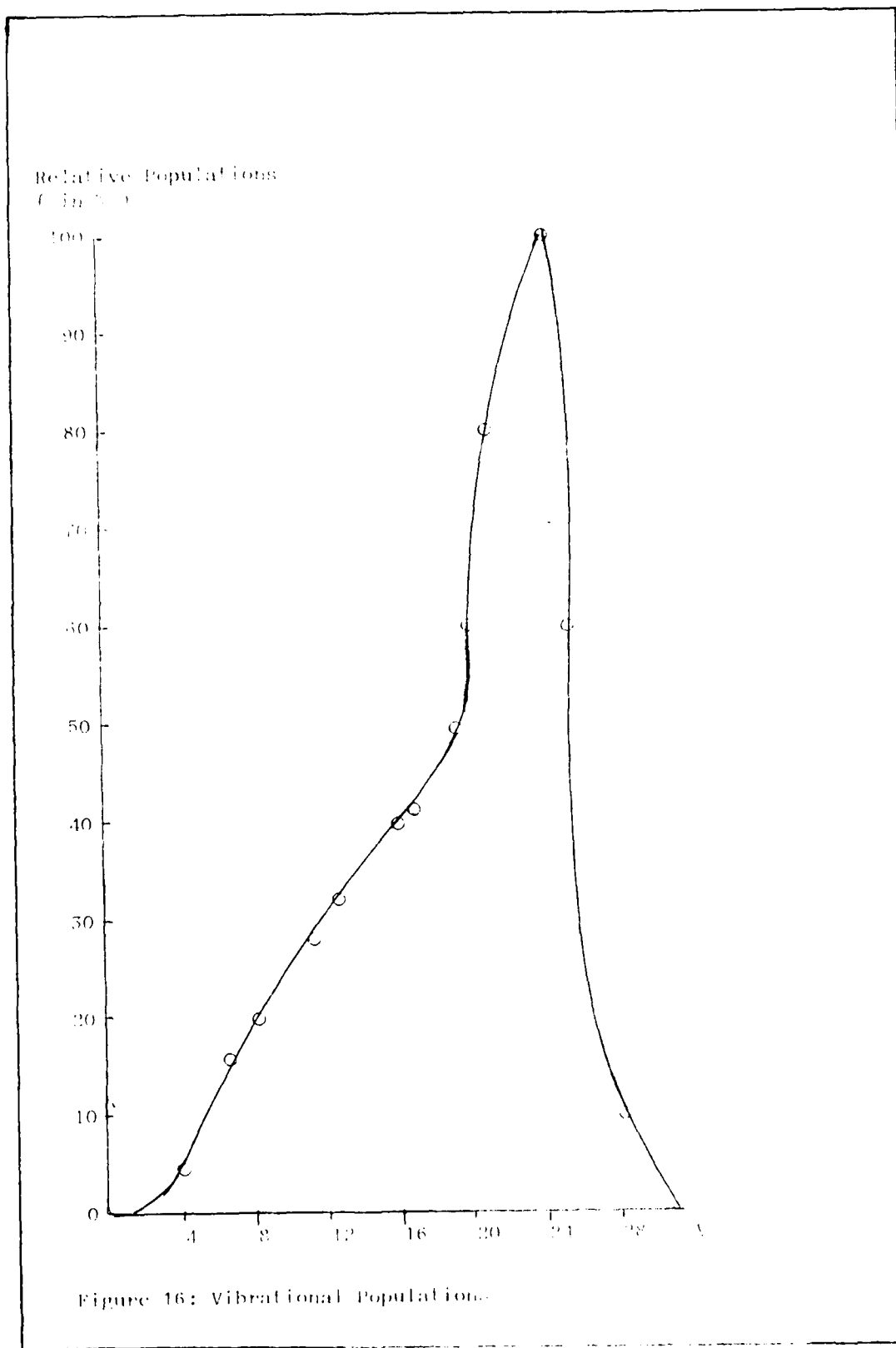
Figure 16 (Ref 16:722). Maximum populations occurred between $v' = 16$ and $v' = 24$. The relative populations were calculated by assuming

$$N_{v'} = R_{v'} + \sum_v k_{v,v'} [O_2] [N_v] \quad (\text{Ref 16:722}) \quad (31)$$

Here $R_{v'}$ is the relative rate of population of the vibrational level of $I_2(B)$ and the $k_{v,v'}$ are the rate coefficients for de-excitation from v' to v (Ref 16:722). The physical significance of these relative populations is that, at room temperature, the majority of the $I_2(B)$ molecules will be in states above $v' = 16$, and a substantial number will be between 8 and 16.

This information helps to predict the bandhead position. The probability distributions for a molecule in the $I_2(B)$ state in the higher vibrational levels are highest for molecules on the extremums; i.e., lying on the potential curve. This situation is schematically represented in Figure 15.

For a transition between the upper and lower electronic states, the Franck-Condon principle states that the electronic transition occurs much faster than the vibrational transition (Ref 5:208). This in effect freezes the vibrational motion of the molecule while the transition occurs, so that after the transition the molecule finds itself with the same internuclear separation r_e . In the lower electronic state,



this r_0 now corresponds to a different probability distribution and hence a different vibrational state v'' .

The probability that a molecule in state $I_2(B), v'$, will end up in state $I_2(X), v''$ in an electronic transition is given by the Franck-Condon factor $g_{v',v''}$. A full discussion of $g_{v',v''}$ is beyond the scope of this thesis, but the basic approach is to calculate the transition matrix element between the upper and lower states for each v', v'' pair. A fuller discussion for the I_2 molecule is presented by Tellinghuisen (Ref 47).

Table IV shows selected Franck-Condon factors for the transitions $v' + v'' = 0$ (Ref 47:153). From the values reported, it can be seen that transitions from $I_2(B)v'$ which terminate in $I_2(X)v'' = 0$ are likely for high v' numbers.

As long as the assumption is made that the upper vibrational levels are more highly populated, as Derwent and Thrush have shown, the following correlation scheme is plausible.

First, the total energy is taken to be

$$E_{\text{total}} = E_{\text{electronic}} + E_{\text{vibrational}} + E_{\text{rotational}} \quad (32)$$

(Ref 5:76)

TABLE IV
Franck-Condon Factors for
 $I_2(B), v' \rightarrow I_2(X), v'' = 0$

| <u>$v' - v''$</u> | <u>Franck-Condon Factor</u> | <u>$v' - v''$</u> | <u>Franck-Condon Factor</u> |
|------------------------------|-----------------------------|------------------------------|-----------------------------|
| 0.0 | 1.4×10^{-9} | 18.0 | 1.2×10^{-2} |
| 1.0 | 2.2×10^{-8} | 19.0 | 1.4×10^{-2} |
| 2.0 | $.17 \times 10^{-7}$ | 20.0 | 1.7×10^{-2} |
| 3.0 | 3.8×10^{-7} | 21.0 | 1.9×10^{-2} |
| 4.0 | 3.5×10^{-6} | 22.0 | 2.2×10^{-2} |
| 5.0 | 1.1×10^{-5} | 23.0 | 2.4×10^{-2} |
| 6.0 | 3.2×10^{-5} | 24.0 | 2.6×10^{-2} |
| 7.0 | 7.8×10^{-5} | 25.0 | 2.8×10^{-2} |
| 8.0 | 1.7×10^{-4} | 26.0 | 3.0×10^{-2} |
| 9.0 | 3.4×10^{-4} | 27.0 | 3.1×10^{-2} |
| 10.0 | 6.2×10^{-4} | 28.0 | 3.2×10^{-2} |
| 11.0 | 1.1×10^{-3} | 29.0 | 3.2×10^{-2} |
| 12.0 | 1.7×10^{-3} | 30.0 | 3.2×10^{-2} |
| 13.0 | 2.6×10^{-3} | 31.0 | 3.2×10^{-2} |
| 14.0 | 3.8×10^{-3} | 32.0 | 3.2×10^{-2} |
| 15.0 | 5.3×10^{-3} | 33.0 | 3.1×10^{-2} |
| 16.0 | 7.1×10^{-3} | 34.0 | 3.0×10^{-2} |
| 17.0 | 9.2×10^{-3} | 35.0 | 2.9×10^{-2} |

The rotational energy will be given by

$$E_{\text{rot}} = B J(J + 1) \text{ cm}^{-1} \quad (\text{Ref 5:33}) \quad (33)$$

and ΔE_{rot} by

$$\Delta E_{\text{rot}} = 2 B(J + 1) \text{ cm}^{-1} \quad (\text{Ref 5:34}) \quad (34)$$

The vibrational energy is given by

$$E_{\text{vib}} = \omega_e (v + 1/2) - X_e \omega_e (v + 1/2) \quad (35)$$

(Ref 5:73)

$$\Delta E_{\text{vib}} \cong \bar{\omega}_e (1 - 2X_e) \quad (\text{Ref 5:73}) \quad (36)$$

For $I_2(B)$, $B = 0.0292 \text{ cm}^{-1}$, $\omega_e = 128.0 \text{ cm}^{-1}$, and $X_e \omega_e = 0.834 \text{ cm}^{-1}$ (Ref 29:541). For these values, $\Delta E_{\text{rot}}/\Delta E_{\text{vib}} = 0.005$. So it is reasonable, to a first approximation, to neglect the rotational energy for band-head assignments.

The assumption is made, based on the Franck-Condon factors, that the transition terminates at $v'' = 0$ in the $I_2(X)$ state. Then the energies of the states are given as follows.

$$\Delta E = T_e + \Delta E v' - \Delta E v'' = 0 \quad (37)$$

For $I_2(B)$, $T_e = 15641.6 \text{ cm}^{-1}$, $\omega_e X_e$, ω_e are as given, and for $I_2(X)$, $T_e = 0$, $\omega_e X_e = 0.6127$, and $\omega_e = 214.57$ (Ref 29:541). Then v'' is assumed to be 0, and the energy of the transition is given by Eq (38).

$$\begin{aligned} E(\text{cm}^{-1}) &= 15641.6 + 128.0(v' + 1/2) \\ &- 0.834(v' + 1/2)^2 - 214.57(1/2) \\ &+ 0.6127(1/2)^2 \\ &= 15534.6 + 128(v' + 1/2) - 0.834(v' + 1/2)^2 \quad (38) \end{aligned}$$

Table V shows the wavelength of the bandheads predicted in this fashion. Figure 17 shows a data record with calculated bandheads shown by circles and identified by v' . The bands shade toward red (Ref 13), so the bandheads should occur on the left shoulder or near the peak of the transitions.

Relative Intensity Plots. Figure 18 shows a plot of the experimental data, corrected for photomultiplier response and absorption, and a plot taken from work by Thrush (Ref 16:721). Corrections for photomultiplier response were made

TABLE V
 Calculated $I_2(B) \rightarrow I_2(x)$ Transitions

| v' | (calculated in \AA°) | v' | (calculated in \AA°) |
|------|-------------------------------------|------|-------------------------------------|
| 5 | 6168 | 21 | 5586 |
| 6 | 6123 | 22 | 5558 |
| 7 | 6080 | 23 | 5530 |
| 8 | 6038 | 24 | 5504 |
| 9 | 5997 | 25 | 5478 |
| 10 | 5957 | 26 | 5452 |
| 11 | 5918 | 27 | 5428 |
| 12 | 5881 | 28 | 5404 |
| 13 | 5844 | 29 | 5381 |
| 14 | 5809 | 30 | 5358 |
| 15 | 5774 | 31 | 5336 |
| 16 | 5741 | 32 | 5315 |
| 17 | 5708 | 33 | 5295 |
| 18 | 5676 | 34 | 5275 |
| 19 | 5645 | 35 | 5256 |
| 20 | 5615 | | |

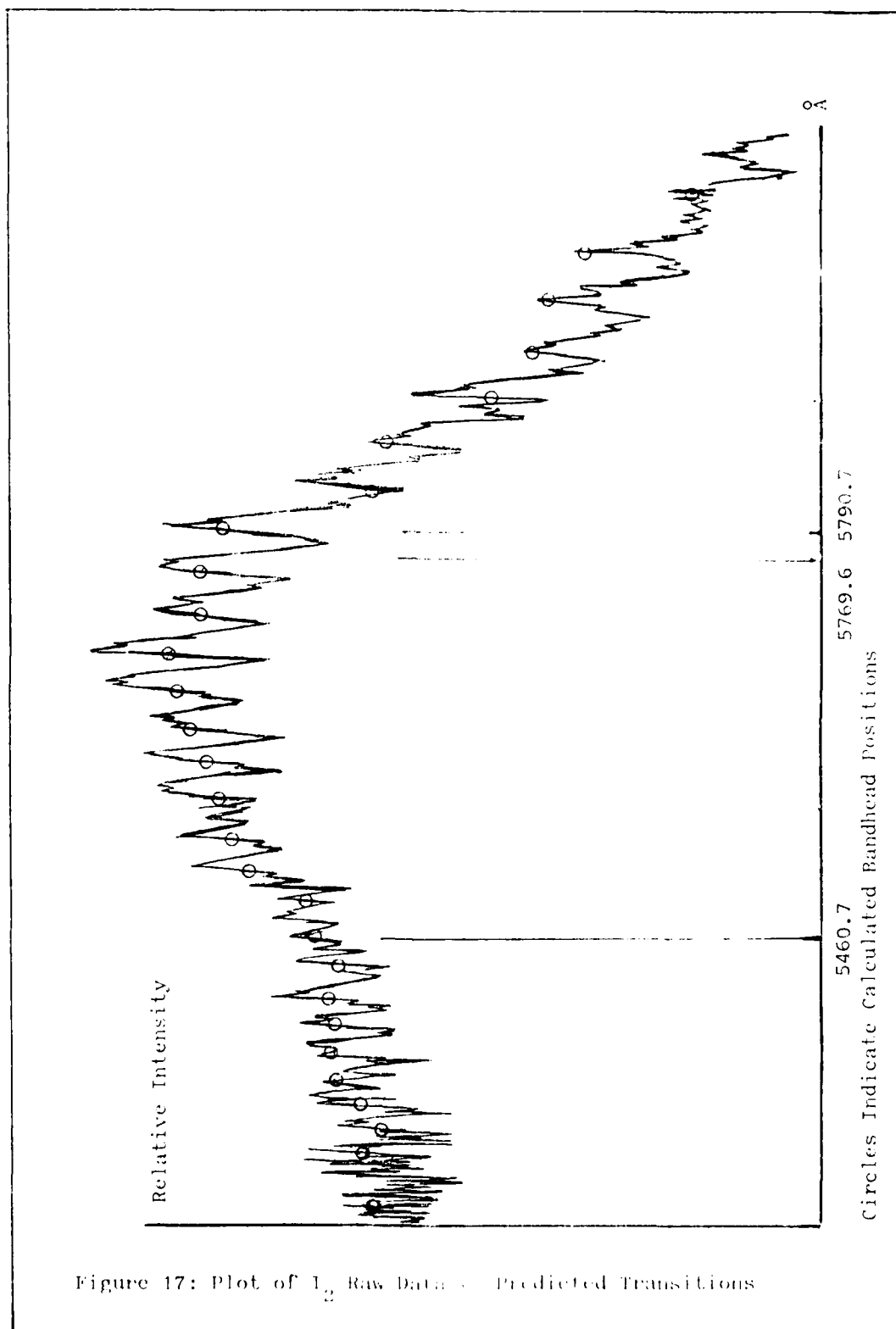


Figure 17: Plot of I_2 Raw Data vs. Predicted Transitions

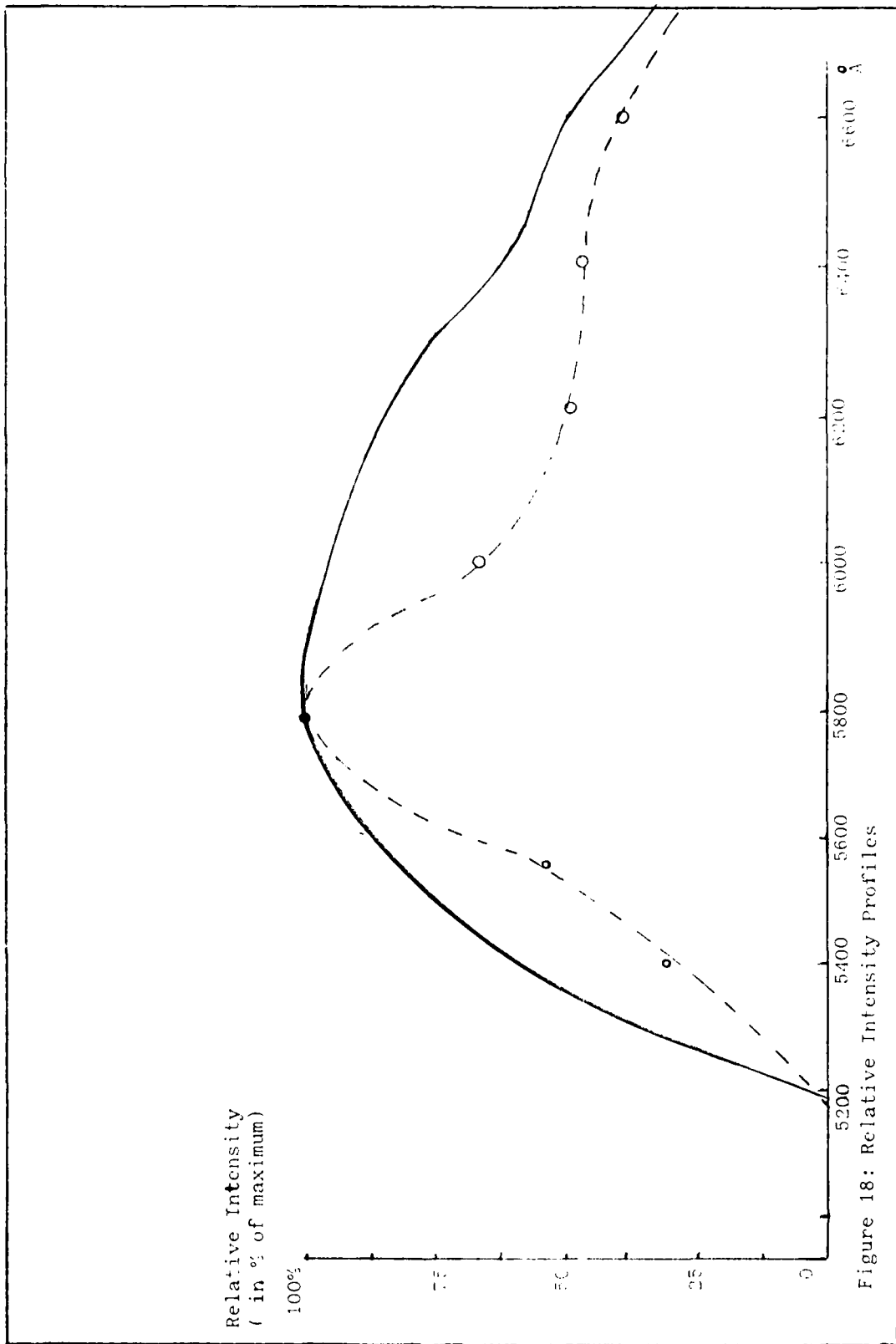


Figure 18: Relative Intensity Profiles

from manufacturer's typical response curves (Ref 39).

Initially, it was assumed that the absorption could be described by assuming that I was proportional to some I_0 times an exponential time dependence. After considerable trial and error, it was decided that the actual behavior could best be described by Eq (39)

$$\alpha(\% \text{ attenuation}) = t \frac{0.4 + [2.3 \times 10^{-4} / \text{\AA}] \times \# \text{ of } \text{\AA} \text{ above } 5100 \text{\AA}}{4.5 \text{ minutes}} \quad (39)$$

where t is in minutes required to sweep from 5100\AA to the wavelength in question, and the monochromator is sweeping in the direction of increasing wavelength. Thus the absorption shows a linear time dependence plus a wavelength dependence. No error estimate is made.

Discussion. The correlation between predicted and observed transitions is excellent up to $\nu' = 30$. Noise above 5300\AA made it difficult to assign transitions above $\nu' = 30$.

The relative intensity plots are less convincing. The lateral symmetry is similar, and the high frequency observation limit ($\sim 5100 \text{\AA} \pm 50 \text{\AA}$) is the same. However, there is a significant difference in the relative intensities across most of the spectrum. Most of the difference can be attributed to differences in the experimental conditions, since the pressures were different ($P_{\text{total}} = 0.35$ torr in this work; 3.4 torr in Derwent and Thrush (Ref 16:720))

and temperature measurements of the flow tube gases were not made in this thesis.

However, based on the correlation between the predicted and observed transitions, it was felt that I_2 chemiluminescence had been demonstrated.

PbO Experiment

Qualitative agreement was obtained with the literature. Table VI lists some of the observations made as a function of experimental parameters.

As Linton and Broida noted in their paper, the plus flame at low pressures was quite weak (Ref 33:408). It was determined that an improvement in the signal to noise ratio of the measurement system was required to yield quantitative results.

A qualitative correlation was obtained between power dissipated in the coil and the reaction products. At wattages below 250 - 300 W, there were no reaction products, and between 300 W and 500 W, the major products were PbO (identified by the yellow color) and Pb_2 plated on the chamber walls. Above 600 W, a black oxide formed; presumably Pb_2O (Ref 28).

TABLE VI

PbO Flame Observations

| <u>N₂O Pressure</u> | <u>Ar Pressure</u> | <u>Voltage</u> | <u>Color Flame</u> | <u>Comments</u> |
|--------------------------------|--------------------|----------------|------------------------|---|
| 0.5 | 6.0 | 13.0 | Blue | Faint but well defined |
| 1.0 | 4.0 | 13.0 | Blue | " " |
| 1.5 | 2.0 | 13.0 | Blue | " " |
| 2.0 | 2.0 | 13.0 | Blue | " " |
| 4.7 | 1.7 | 13.5 | Blue | Very faint |
| 0.1 | 4.0 | 14.0 | Blue | Excellent flame, little fouling, bright, well-formed flame |
| 4 - 5 | 0 - 2 | 14.7 | Blue | Well-formed flame, much black oxide |
| 2.0 | 10.0 | 14.0 | Yellow | High following |
| 2.5 | 4.5 | 14.5 | Yellow | Wire burnt in two |
| 10.0 | 15.0 | 14.5 | Yellow | " |
| 10.0 | 20.0 | 14.4 | Yellow | " |
| 30 | Off-Scale | 18.0 | Yellow | " |

VI. Conclusions and Recommendations

Flow Tube Performance

A working gas flow tube was demonstrated. Experiments were conducted in the laminar flow regime from 0.35 to 30.0 mm pressure. The capability to do oxidation, excited gas, and high temperature metal vapor reactions was demonstrated.

Experiments

I₂/O₂ Chemiluminescence. This experiment demonstrated the use of a microwave power source to generate singlet molecular oxygen. The experiment reproduced data acquired by previous researchers and agreed with theoretical calculations of predicted emissions. It was concluded that the emissions were consistent with emission from the I₂ (³Π_{o+u}⁺ → ³Π_g) transition in iodine.

Pb + N₂O. Severe problems with gas dynamics and chamber fouling were solved, and a qualitative observation of the flame was made. This observation was in agreement with descriptions of the flame in the literature. Equipment problems with the measuring system prevented the acquisition of quantitative data.

Recommendations

Several improvements to the flow can be made, and follow-on experiments are suggested in this section.

Gas Flow Tube. A length of 3.0 inch inner diameter transparent tube should be purchased for installation in the transition section. The tube should be of quartz because of the superior transmission properties of quartz in the ultraviolet spectrum. This modification will allow gas kinetic studies to be performed in this tube. Electrodes should be made for the combustion chamber to allow spark discharge studies to be performed.

Furnace. Additional hood shapes should be investigated such as the one shown in Figure 19. The goal should be to

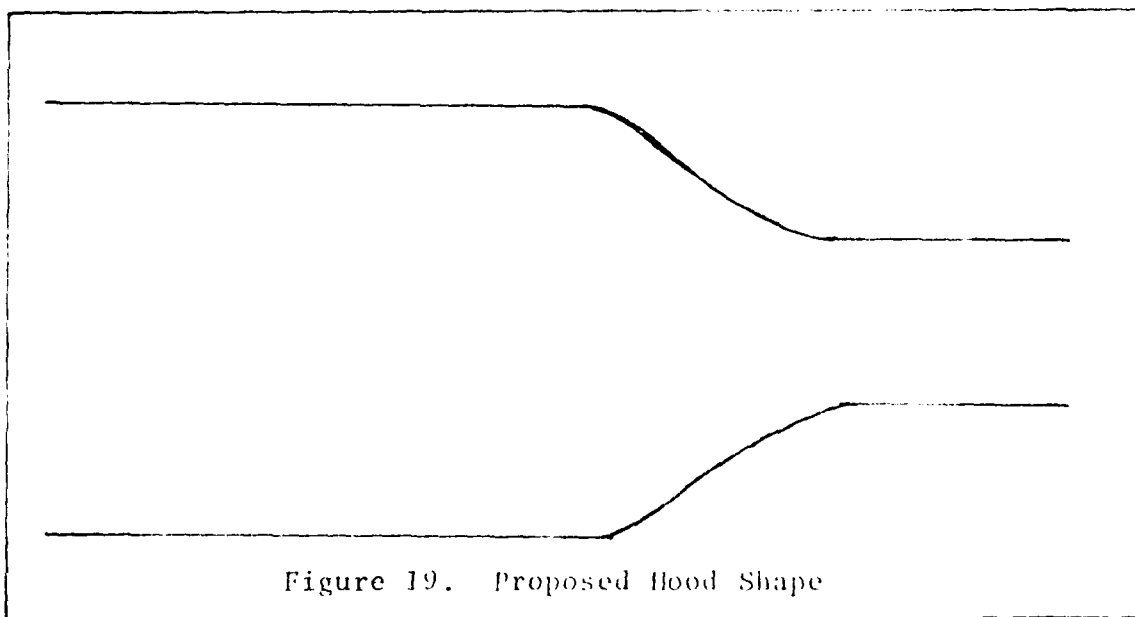


Figure 19. Proposed Hood Shape

obtain the most efficient flow of metal into the combustion chamber with the least deposition in the furnace. Figure 19 shows a proposed method for eliminating recirculation in the furnace chamber. The hood should be configured with a heating wire on the outside of the hood. This design would allow the hood to be heated and thus prevent plating of the vapor from the furnace on the inside of the hood.

Another possibility is a new furnace designed such as the one in Figure 20. The object would be to avoid recirculation or combustion ahead of the viewing area, while simplifying recharging procedures and avoiding fouling problems.

Measurement System. The most obvious way for improving the flow tube would be to improve the measurement system. Two approaches are recommended.

Viewing Arrangements. The present arrangements require a viewing path of 2 to 3 feet to avoid plating. This cuts down the signal intensity, and so a way to shorten the view path is required. Figure 21 shows an insert to be placed in the tube ahead of the viewing window, which would create a uniform gas blanket over the window to prevent deposition (Ref 13). This should allow the view port to be placed adjacent to the combustion chamber.

When studying the rate coefficients of a reaction, it may not be possible to use a flushing gas. For these circumstances, the modification in Figure 22 is

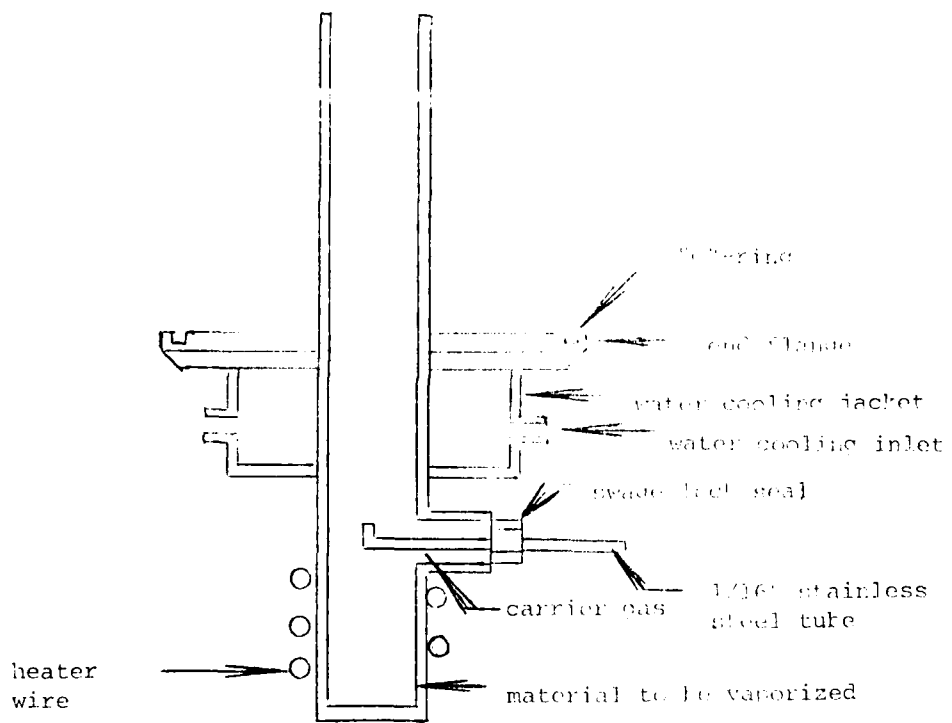


Figure 20: Proposed Furnace

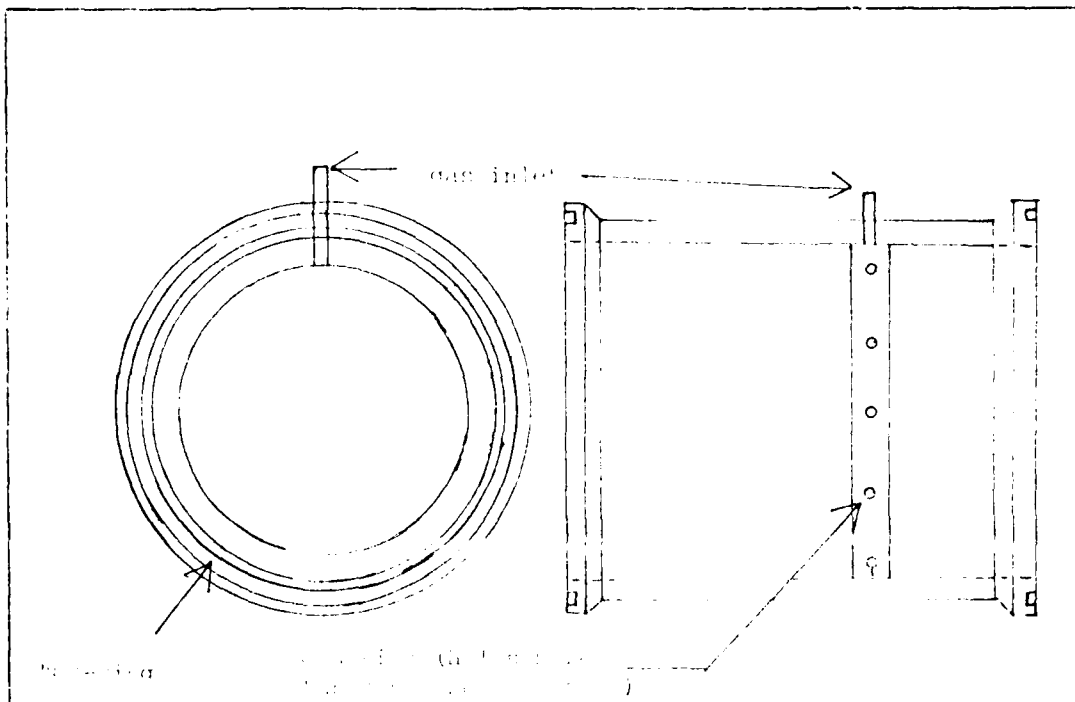


Figure 21: Gas Inlet Detail

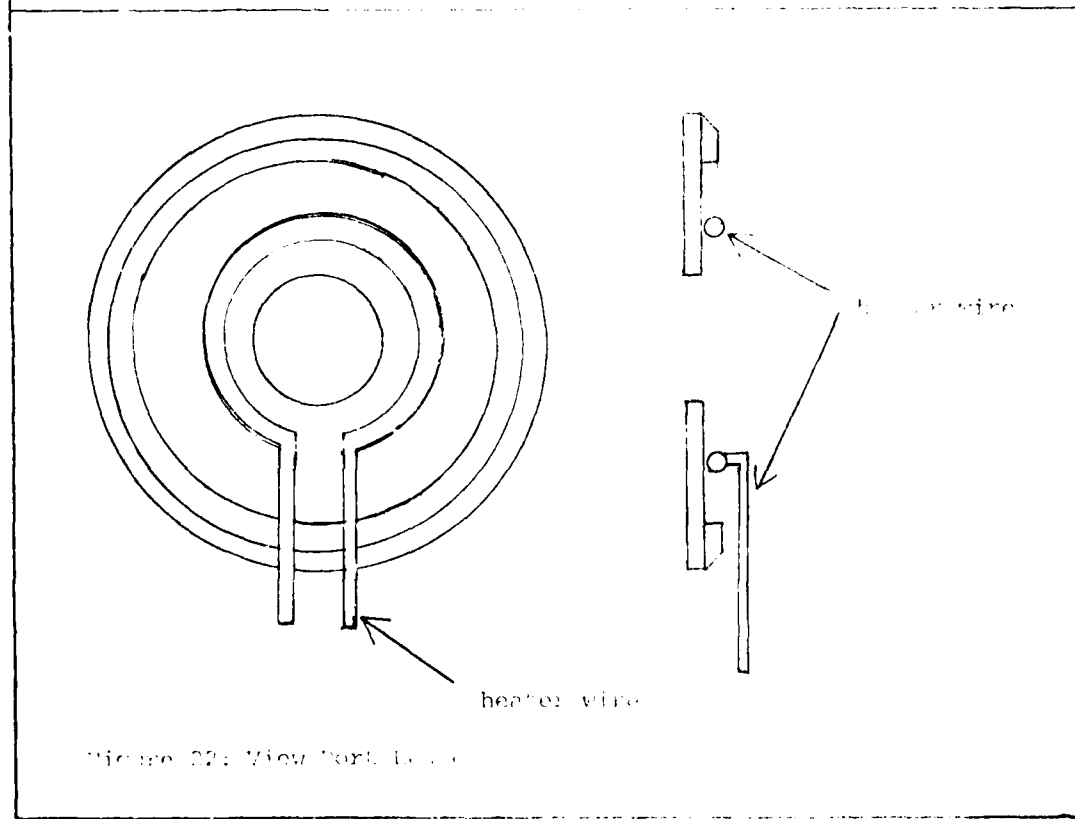


Figure 22: View Port Detail

proposed. The object would be to prevent deposition of compounds such as I_2 which have low vaporization temperatures.

Electrical Noise Reduction. The electrical noise problems encountered on this thesis should be solvable. One possibility is to electrically isolate the photomultiplier from the monochromator. According to Dr. Won Roh of the AFIT faculty, this is a major source of noise. A second possibility is to cool the 7265 to reduce thermionic emission. This would require fabrication of a cooling collar and selection of a cooling medium.

Experiments

PbO. With a new measurement system available, research should continue on the PbO reaction. A possible approach would be to enhance the PbO spectra by excitation with excited nitrogen or singlet molecular O_2 . Linton and Broida (Ref 33:409) showed that the addition of active nitrogen to a $Pb + N_2O$ flame strongly enhanced the $A \rightarrow X$, $B \rightarrow X$, $C \rightarrow X$, and $D \rightarrow X$ systems, with some individual transitions between 6000 and $4000\overset{\circ}{\text{A}}$ being 30 times as intense. Additionally, N_2^* excited some atomic Pb transitions; probably the 1S_0 state. An obvious approach would be to use the microwave to produce active N_2 or O_2 ($^1\Delta$ or $^1\Sigma$) and record the spectra. Then radiative lifetime measurements can be made on the most strongly excited states to determine if a likely candidate system exists for establishing a population inversion.

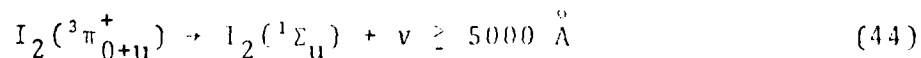
An additional area for investigation was suggested by Davis (Ref 13). The spectra enhanced by active nitrogen (Ref 33:408) show evidence of excitation to excited states of the Pb molecule. Davis suggests that the $\text{PbO} + \text{N}_2^*$ reaction be used as an energy transfer mechanism to excite the $^1\text{S}_0 \rightarrow ^3\text{P}_1$ or $^1\text{D}_2 \rightarrow ^3\text{P}_1$ atomic transitions of Pb (Ref 13). With rate constants of 88/sec and 26 sec, respectively, these metastable states may be good candidates for a visible laser.

Testing this hypothesis would require measuring the rate constants for the reactions



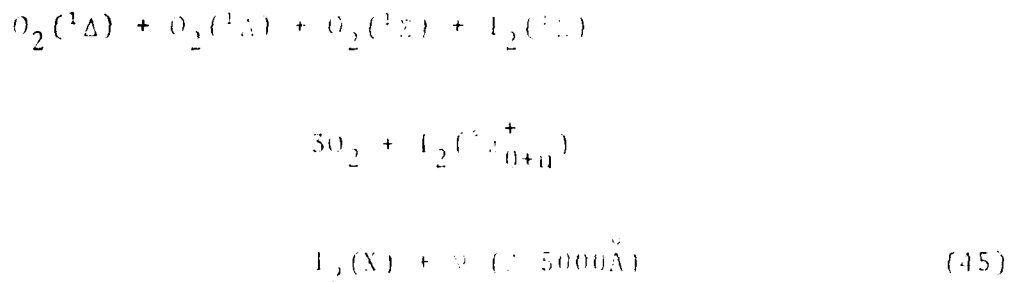
and other paths.

I₂ Chemiluminescence Models. Several models have been proposed to explain the I₂ chemiluminescence. There is general agreement that the bright yellow-green glow resulting from introducing I₂ molecules into a stream of O₂(¹Δ) and O₂(¹Σ) molecules is due to the transition (Ref 16:720)



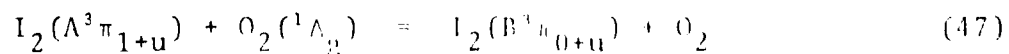
However, there is no general agreement on the nature of the excitation mechanism. Arguments put forth by Arnold, Finlayson, and Ogryzlo (Ref 2:2529) represent earlier views. However, later work by Derwent and Thrush (Ref 16:721) represents a radically different view of the mechanism.

Arnold et al. (Ref 2:2530) hypothesized a recombination scheme:

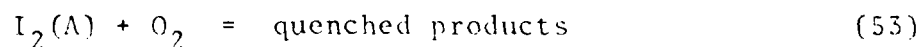
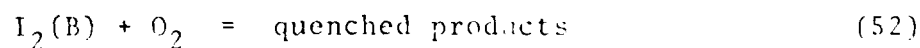
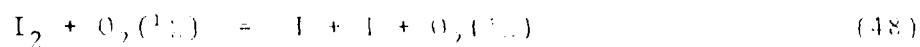


This reaction, as reported, requires a three body reaction to proceed, resulting in a second or third order intensity dependence on the concentration of $O_2(^1\Delta)$. This relationship does not appear to hold, based on the work done by Detwent and Thrush.

Derwent and Thrush report a second possibility, that of stepwise excitation via the following processes:

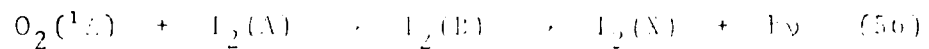
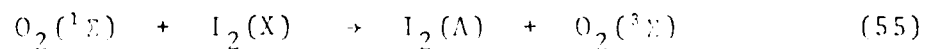
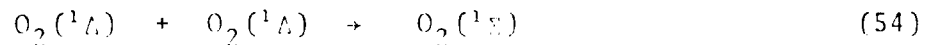


Their argument is based on the vibrational levels populated and the spatial distribution of the luminescence in their flow tube (Ref 16:115). In a later paper, Derwent et al. present evidence that the I_2 chemiluminescence is dependent on the first power of the iodine concentration (i.e., a plot of relative intensity of the chemiluminescence vs. pressure is linear) (Ref 16:724). Based on the linear behavior of the intensity, Derwent and Thrush proposed the following total mechanism to account for the chemiluminescence.



Russell and Simons (Ref 41:271) showed that the process $I + I + O_2 = I_2 + O_2$ is too slow to compete with the diffusion controlled wall removal of iodine, and so does not contribute to the reaction rates.

The various theories of this chemiluminescence need to be investigated. If the hypotheses of Derwent and Thrush are correct, the chemiluminescence is the result of



This contention could be tested as follows. First, establish $[O_2(^1\Delta)]$. The $[O_2(^1\Delta)]$ can be determined by comparing the intensity of 1.27 μ radiation from $O_2(^1\Delta)$ with the total gas flow (Ref 48:299). If Derwent and Thrush are correct, the rate of formation of $I_2(A)$ should depend on the second power of the $[O_2(^1\Delta)]$, or the first power of $[O_2(^1\Sigma)]$. The $[O_2(^1\Sigma)]$ can be determined by observing the intensity of emission at 1.91 μ . If the chemiluminescent intensity is dependent on the first power of $O_2(^1\Delta)$, $O_2(^1\Sigma)$, and $I_2(A)$, this would be excellent evidence for the theory of Derwent and Thrush.

Gas Dynamics

The flow patterns in various parts of the flow tube should be observed by means of smoke streams in order to aid in the design of a more efficient flow tube system.

Bibliography

1. Anderson, R.A., L. Hanko, and S.J. Davis. "Time Resolved Fluorescence of the $\Lambda^2\Sigma^+$ State of GeI." Journal of Chemical Physics, 68: 7 (April 1978).
2. Arnold, S.J., N. Finlayson, and E.A. Ogryzlo. "Some Novel Energy-Pooling Processes Involving $O_2(^1\Delta_g)^*$." Journal of Chemical Physics, 44: 2529 (April 1966).
3. Arnold, S.J., E.A. Ogryzlo, and H. Witzke. "Some New Emission Bands of Molecular Oxygen." Journal of Chemical Physics, 40: 1769 (March 1964).
4. Atomic Energy Levels, Vol. III. Circular 467, USDC-NBS, Washington DC: National Bureau of Standards, 1958.
5. Banwell, C.N. Fundamentals of Molecular Spectroscopy. (Second Edition) London: McGraw-Hill, 1972.
6. Barrow, R.F., E.E. Vago, et al. "Discussion on band Spectra." Proceedings of the Physics Society of London, 56: 208-211 (May 1944).
7. Barrow, R.F. and E.E. Vago. "Ultra-violet Absorption Band-Systems of PbO, PbS, PbSe, and PbTe." Proceedings of the Physics Society of London, 81: 705 (April 1963).
8. Barrow, R.F., P.W. Fry, and C. LeBargy. "Rotational Analysis of the Absorption Spectrum of PbS." Proceedings of the Physics Society of London, 81: 705 (April 1963).
9. Barrow, R.F. Introduction to Molecular Spectroscopy. New York: McGraw-Hill Publishing Co., 1962.
10. Bloomenthal, S. "Vibrational Quantum Analysis and Isotope Effect for the Lead Oxide Band Spectra." Physical Review, 35: 34-45 (January 1930).

11. Brown, R.L. "Tubular Flow Reactors with First-Order Kinetics." Journal of Research of the National Bureau of Standards, 83(1): 1-8 (Jan-Feb 1978).
12. Bugrim, E.N., S.N. Makernko, and I.L. Tsikora. "Efficiency of the Vibration Deactivation and Quenching of the Electronically Excited I_2 Molecule." Optical Spectroscopy, 37(6): 610-612 (December 1974).
13. Davis, S.J, private communication, 1980.
14. Davis, S.J. and S.G. Hadley. "Measurement of the Radiative Lifetime of the A^2 ($v'=0$) State of Si F." Physical Review A, 14(3): 1146-1150 (September 1976).
15. Derwent, R.G. and B.A. Thrush. "Measurements on $O_2(^1\Delta_g)$ and $O_2(^1\Sigma_g^+)$ in Discharge Flow System." Transactions of the Faraday Society, 67: 2036-2043 (July 1971).
16. Derwent, R.G. and B.A. Thrush. "Excitation of Iodine by Singlet Molecular Oxygen." Transactions of the Faraday Society, : 720-728.
17. Derwent, R.G., D.R. Kearns, and B.A. Thrush. "The Excitation of Iodine by Singlet Molecular Oxygen." Chemical Physics Letters, 6(2): 115-116 (July 1970).
18. Electro-Optics Handbook. RCA Defense Electronics Products/Aerospace Systems Division. Massachusetts, 1968.
19. Dorko, Ernest A. Lecture materials distributed in PH 6.61, Methods of Spectroscopy. School of Engineering, Air Force Institute of Technology, Wright-Patterson AFB, OH, 1979.
20. Evenson, K.M., J.L. Dunn, and H.P. Broida. "Optical Detection of Microwave Transitions Between Excited Electronic States of CN and the Identification of the Transitions Involved." Physical Review, 136(6A): A1566-1568 (December 1964).

21. Fontijn, A., W. Felder, and J.J. Houghton. "Tubular Fast-Flow Reactor Studies at High Temperatures. Kinetics of the Al/O₂ Reaction." Chemical Physics Letters, 27(3): 365-368 (August 1974).
22. Fontijn, A. and S.C. Kurzius. "Tubular Fast-Flow Reactor Studies at High Temperatures. Kinetics of the Fe/O₂ Reaction at 1600° K." Chemical Physics Letters, 13(5): 507-510 (April 1972).
23. Fontijn, Arthur. Kinetic Spectroscopy of Metal Atom/Oxidizer Chemiluminescent Reactions for Laser Applications. Interim Report for Period 1 May 1976 - 30 April 1977; Aero Chem TN-175. Washington DC: Air Force Office of Scientific Research, Bolling AFB DC.
24. Fontijn, A. and W. Felder. "High Temperature Fast-Flow Reactor Study of Sn/N₂O Chemiluminescence." Chemical Physics Letters, 54(2): 398-402 (May 1972).
25. Fontijn, A., et al. "Tubular Fast Flow Reactor for High Temperature Gas Kinetic Studies." Review of Scientific Instruments, 43(5): 720-724 (May 1972).
26. Hagar, G., et al. "Reactions of Atomic Silicon and Germanium with Nitrous Oxide to Produce Electronically Excited Silicon Monoxide and Germanium Oxide." Chemical Physics Letters, 27(3): 439-441 (August 1974).
27. Hagar, G., et al. The $a^3\Sigma^+ \rightarrow X^1\Sigma^+$ and $b^1\Pi \rightarrow X^1\Sigma^+$ Band Systems of SiO and the $a^3\Sigma^+ \rightarrow X^1\Sigma^+$ Band System of GeO Observed in Chemiluminescence." Journal of Chemical Physics, 63(7): 2810-2820 (October 1975).
28. Handbook of Chemistry and Physics, (Fiftieth Edition). Cleveland: The Chemical Rubber Company, 1970.

29. Herzberg, G. Spectra of Diatomic Molecules, (Second Edition). New York: Reinhold Co., 1950.
30. Instruction Manual, Model 82-000 0.5 Meter Ebert Scanning Spectrometer. Jarrel-Ash Division/Fisher Scientific Co., Waltham MA, 1971.
31. Thermo-Chemical Tables, Second Edition. USDC-NBS, JANAF Washington DC: National Bureau of Standards, 1971. SN0303-0872.
32. LeRoy, Robert. "Spectroscopic Reassignment and Ground-State Dissociation Energy of Molecular Iodine." Journal of Chemical Physics, 52(5): 2678-2682 (March 1970).
33. Linton, C. and H.P. Broida. "Chemiluminescent Spectra of PbO from Reactions of Pb Atoms." Journal of Molecular Spectroscopy, 62: 390-415 (September 1976).
34. McDermott, W.E., N.R. Pchelkin, D.J. Bernard, and R.R. Bousele. "An Electronic Transition Chemical Laser." Applied Physics Letters, 32(8): 469-470 (April 1978).
35. Nair, K.P.R., R.B. Dingham, and D.K. Rai. "Potential Energy Curves and Dissociation Energies of Oxides and Sulfides of Group IVA Elements." Journal of Chemical Physics, 43: 3570-3574 (November 1965).
36. Oldenberg, R.C., et al. "A New Electronic Band System of PbO." Journal of Molecular Spectroscopy, 58: 283-300 (November 1975).
37. Oriel Spectrophotometer Calibration Set Model C-13-02. Product Brochure. Stamford CT: Oriel Optics Corp.
38. Pennucci, M.A. "Parametric Evaluation of Total Pressure Loss and Recirculation Zone Length in a Sudden Expansion Combustor." Unpublished MS Thesis, School of Engineering, Department of Aeronautics and Astronautics, Air Force Institute of Technology, Wright-Patterson AFB OH, September 1974.

39. RCA Tube Handbook, HB-3. Harrison NJ: 1967.
40. Roth, A. Vacuum Technology. New York: North-Holland Publishing Company, 1976.
41. Russell, K.E. and J. Simons. "Studies in Energy Transfer. J* The Combustion of I Atoms." Proceedings of the Royal Society A, 217: 271 (April 1953).
42. Sax, N.I. Dangerous Properties of Industrial Material, Third Edition. New York: Reinhold Press, 1968.
43. Shawhan, E.N. and F. Morgan. "Absorption Spectrum of Lead Oxide." Physical Review, 47: 377-378 (March 1935).
44. Steinfeld, J.I. Molecules and Radiation: An Introduction to Molecular Spectroscopy, 88. Cambridge MA: MIT Press, 1978.
45. Suchard, S.N. Spectroscopic Data for Heteronuclear-Diatomic Molecules, Vol. II. Plenum Publications, 1975.
46. Swearingen, P.M., et al. "Reaction Rate Studies of Atomic Germanium ($^3P_{0,1}$) and Silicon (3P_J) with Various Oxidizers." Chemical Physics Letters, 55(2): 274-279 (April 1978).
47. Tellinghuisen, Joel. "Intensity Factors for the $I_2(B) \rightarrow I_2(X)$ Band System." Journal of Quantitative Spectroscopy and Radiative Transfer, 19: 149-161 (June 1977).
48. Thomas, R.G.O. and B.A. Thrush. "Energy Transfer in the Quenching of Singlet Molecular Oxygen, Parts I-III." Proceedings of the Royal Society of London A, 356: 287-314 (September 1977).
49. Thrush, B.A. "Atomic Reactions in Flow Tubes." Science, 154: 470-473 (April 1967).

50. Trajmar, S., D.C. Cartwright, and W. Williams.
"Differential and Integral Cross Sections for the
Electron-Impact Excitation of the $a^1\Lambda_g$ and $^1\Sigma_g^+$ States
of O_2 ." Physics Review A, 4(4): 1482-1492 (October 1971).
51. Vincenti, W.G. and C.H. Kruger. Introduction to
Physical Gas Dynamics. New York: Robert E. Krieger
Publishing Company, 1975.
52. West, J.B., R.S. Bradford, J.D. Eversole, and C.R. Jones.
"Flow System for the Production of Diatomic Metal Oxides
and Halides." Review of Scientific Instruments, 46:
164-168 (February 1975).
53. Wolf, Paul J. The Validity of Velocity Calculations
Based on the Plug Flow Assumption in Flow Tube
Applications. MS Thesis, Wright-Patterson AFB OH:
Air Force Institute of Technology, December 1979.

APPENDIX A

Flow Tube Procedures

Start Up Procedures

General Procedures

1. Close all vacuum fittings.
2. Shut off ball valve to vacuum pumps.
3. If using furnace, replace glass wool in particulate trap, charge furnace with material to be vaporized.
4. Turn on vacuum pumps.
5. Slowly open ball valve.
6. Turn on vacuum pump to reference side of Baratron gauge.
7. When pressure in flow tube (static gauge) is 200 microns, open valve to Baratron gauge and pump for 1 hour.
8. Start Bake function on Baratron at 5, continue till red bake light goes off, then set Bake function switch to regular.
9. When using materials which must be plated out before reaching the vacuum pumps, prepare the cold trap.
 - a. When using oxygen, use a methyl chloride/dry ice slush to cool the cold trap.
DO NOT USE LN2 AS THIS WILL CREATE LIQUID O2 IN THE COLD TRAP!!!
 - b. With other reactions, use LN2.

Microwave Procedures

1. Turn on flow of gas to be excited (0.5 mm for O₂).
2. Turn on microwave generator.
3. After 3 minutes, turn on forward power to 100W. If plasma does not ignite, use a Tesla coil just upstream of the microwave cavity as an additional electron source. Tune with coarse control until plasma is ignited.
4. DO NOT allow power to remain on longer than 5 minutes with the SWR 3, where

$$\text{SWR} = \frac{1 + \sqrt{\frac{\text{reflected power}}{\text{forward power}}}}{1 - \sqrt{\frac{\text{reflected power}}{\text{forward power}}}}$$

5. Turn on microwave cooling gas. Adjust flow until exiting gas is slightly warm to touch.

Furnace Procedures

1. Charge with material to be vaporized.
2. Turn on cooling water.
3. Ensure tube is grounded.
4. Turn on carrier gas.
5. Turn on power.
6. Adjust current to desired vapor temperature.

Shut Down Procedures

1. If using furnace, turn off power. Continue carrier flow and water flow. Short tube surface with ground wire.
2. Shut off power, HV, and power-on switch on microwave.
3. Shut off active gas.
4. Shut gauge connecting Baratron to system.
5. Shut off carrier after 5 minutes.
6. Shut off water after 15 minutes.
7. Shut ball valve off, vent pumps through pump vent valve.
8. Ensure all power off.
9. Leave tube under vacuum.

DO NOT TURN ON FURNACE WITHOUT COOLING WATER ON;

DO NOT TURN OFF COOLING WATER BEFORE TURNING OFF FURNACE!!!

APPENDIX B

Pictures of Apparatus



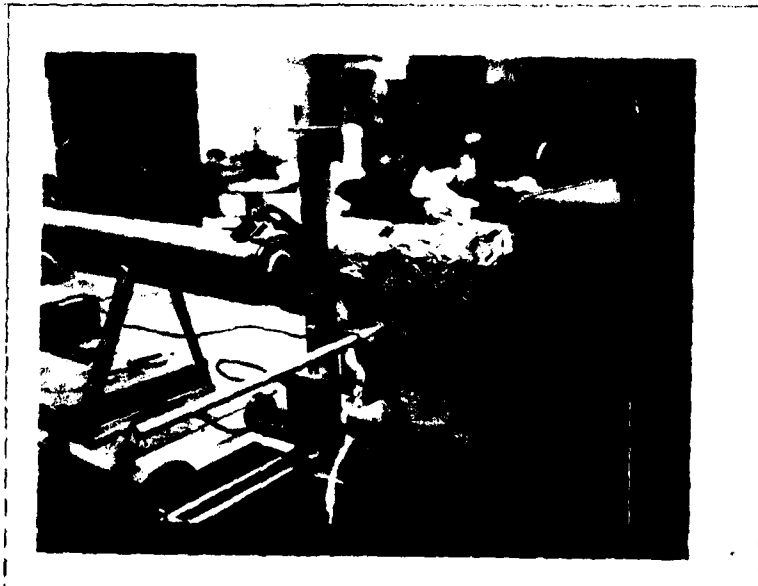
Flow Tube



Microwave Generator and Cavity



Vacuum System



Measurement System and Viewport

APPENDIX C

Useful PbO Data^a

I. $\Lambda O^+ == X^1\Sigma^+$ System

Bandheads in emission

| v',v'' | λ | Intensity | v',v'' | λ | Intensity |
|----------|-----------|-----------|----------|-----------|-----------|
| 3.8 | 6433.63 | 3 | 0.4 | 5910.74 | 6 |
| 0.6 | 6427.73 | 3 | 0.3 | 5677.78 | 6 |
| 2.7 | 6342.01 | 3 | 2.4 | 5617.65 | 3 |
| 1.6 | 6250.75 | 5 | 0.2 | 5459.38 | 6 |
| 0.5 | 6160.52 | 4 | 1.2 | 5331.11 | 3 |
| | | | 1.1 | 5138.18 | 3 |

II. $B1 == X^1\Sigma^+$ System

Bandheads in emission

| v',v'' | λ | Intensity | v',v'' | λ | Intensity |
|----------|-----------|-----------|----------|-----------|-----------|
| 0.5 | 5353.82 | 3 | 0.1 | 4657.98 | 5 |
| 0.4 | 5162.31 | 6 | 1.1 | 4553.71 | 6 |
| 0.3 | 4983.79 | 6 | 1.0 | 4410.38 | 5 |
| 0.2 | 4816.90 | 6 | 2.0 | 4317.06 | 4 |
| | | | 3.0 | 4229.01 | 4 |

III. $CO^+ == X^1\Sigma^+$ System

Bandheads in absorption

| v',v'' | λ | Intensity | v',v'' | λ | Intensity |
|----------|-----------|-----------|----------|-----------|-----------|
| 2.1 | 4156.20 | 3 | 4.0 | 3877.85 | 8 |
| 2.0 | 4037.63 | 3 | 6.1 | 3838.24 | 2 |
| 4.1 | 3987.70 | 4 | 5.0 | 3804.94 | 6 |
| 3.0 | 3955.04 | 7 | 6.0 | 3735.94 | 1 |
| 5.1 | 3910.30 | 3 | 7.0 | 3669.63 | 3 |
| | | | 8.0 | 3607.35 | 1 |

^a λ in Å

IV. C⁻¹ == X¹Σ⁺ System

In absorption, the bandheads form a single intense progression with $v'' = 0$. v' numbering is deduced from isotopic studies.

| | | |
|---------|--------|--------|
| $v'v''$ | 6.0 | 7.0 |
| | 3612.8 | 3554.8 |

V. D1 == X¹Σ⁺ System

Bandheads in emission

| | | | | | |
|-----------|---------|---------|---------|---------|---------|
| v',v'' | 0.2 | 0.1 | 1.1 | 1.0 | 2.0 |
| λ | 3485.68 | 3401.92 | 3341.83 | 3264.36 | 3209.22 |
| Intensity | 6 | 5 | 2 | 2 | 2 |

VI. EO⁺ == X¹Σ⁺ System

In emission, bands with $v' = 1$ are not observed.

Bandheads in absorption

| v',v'' | λ | Intensity | v',v'' | λ | Intensity |
|----------|-----------|-----------|----------|-----------|-----------|
| 1.3 | 3062.67 | 4 | 3.2 | 2925.64 | 3 |
| 2.3 | 3023.38 | 2 | 2.1 | 2900.21 | 4 |
| 1.2 | 2998.52 | 4 | 4.2 | 2894.21 | 1 |
| 2.2 | 2960.73 | 3 | 3.1 | 2866.17 | 5 |
| 1.1 | 2936.19 | 2 | 4.1 | 2836.57 | 1 |
| | | | 3.0 | 2808.5 | 1 |

^a λ in Å

SPECTROSCOPIC CONSTANTS

| State | T_e^a | ω_e^a | $X_e \omega_e^a$ | B_e^a | $a \text{ ex } 10^3{}^b$ | $D \text{ ex } 10^6{}^b$ | r_e^c |
|---------------|---------|--------------|------------------|----------|--------------------------|--------------------------|---------|
| EO^+ | 34455 | 454.1 | 6.95 | 0.2421 | 2.6 | 0.283 | 2.165 |
| D1 | 30194 | 530.4 | 2.9 | 0.2710 | 2.8 | 0.283 | 2.047 |
| C^1 | 24947 | 494 | 3.0 | 0.2491 | 1.8 | 0.25 | 2.135 |
| CO^+ | 23820 | 532 | 3.9 | 0.2545 | 2.1 | 0.25 | 2.112 |
| B1 | 22289 | 489 | | 0.2619 | 2.6 | 0.30 | 2.071 |
| AO^+ | 19862.3 | 444.2 | 0.46 | 0.2588 | 1.4 | 0.33 | 2.095 |
| $X^1\Sigma^+$ | 0 | 721.46 | 3.53 | 0.307519 | 1.9167 | 0.22 | 1.92181 |

Dissociation energy -3.87 ± 0.05 ev, 89 kcal/mole, 31214 cm^{-1}

(Ref 44)

a cm^{-1}

b ev

c \AA

APPENDIX D

Response Curves for Photomultiplier Tubes

This section summarizes some important characteristics of the photomultiplier tubes used in this thesis. The accompanying graphs are typical relative sensitivity curves, and actual tube response may vary $\pm 10\%$.^a

1P21

| | |
|--|---------------------------------|
| Typical anode sensitivity @ 4000Å ^o ----- | 1.2 x 10 ⁵ A/W |
| Typical cathode sensitivity @ 4000Å ^o ----- | 0.04 |
| Current amplification----- | 3.0 x 10 ⁶ A/W |
| Anode dark current----- | 0.1 - 1.0 x 10 ⁻⁸ W |
| Equivalent anode dark current input----- | 0.5 - 5.0 x 10 ⁻¹³ W |
| Equivalent noise input----- | 0.4 x 10 ⁻¹⁶ W |

7265

| | |
|--|---------------------------|
| Typical anode sensitivity @ 4200Å ^o ----- | 3.0 x 10 ⁶ A/W |
| Typical cathode sensitivity @ 4200Å ^o ----- | 0.064 |
| Current amplification----- | 4.8 x 10 ⁷ |
| Anode dark current----- | 5.0 x 10 ⁻⁸ |
| Equivalent anode dark current input----- | 1.2 x 10 ⁻¹³ W |
| Equivalent noise input----- | 2.1 x 10 ⁻¹⁵ W |

^a Figures taken from Reference 59.

100

Relative Sensitivity (%)

1P21 PMT

10

1

2500

3000

3500

4000

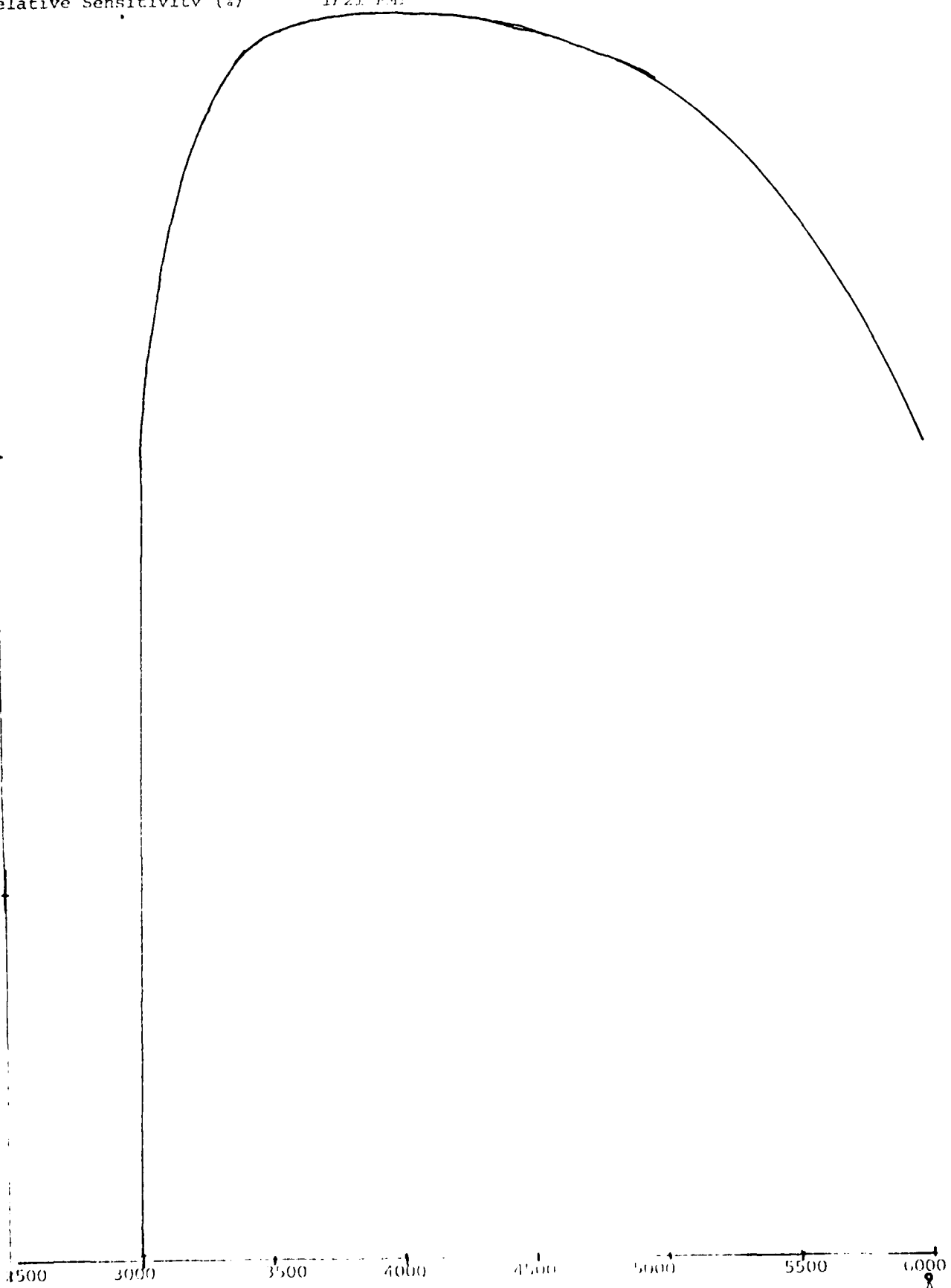
4500

5000

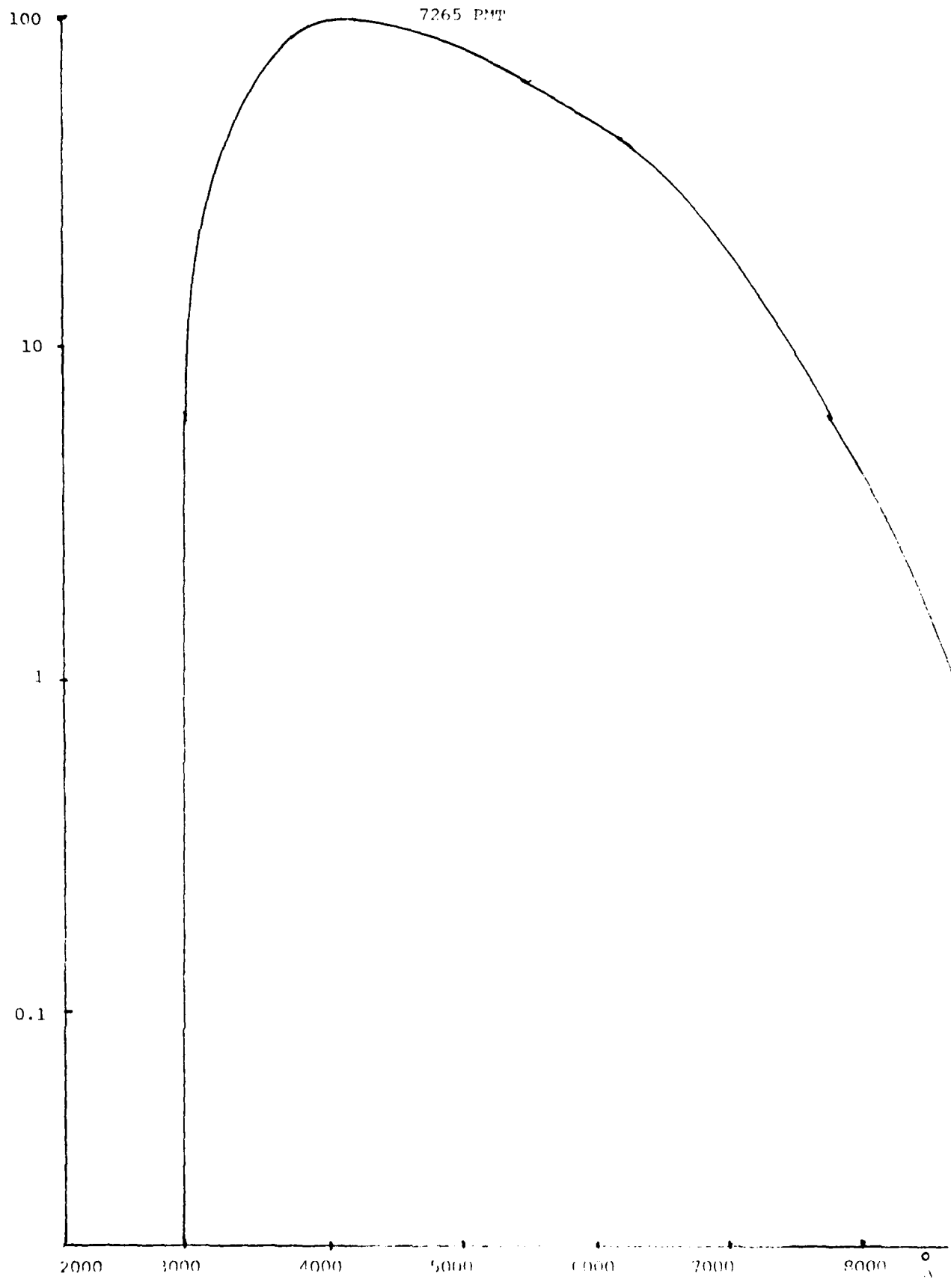
5500

6000

Å



Relative Sensitivity (%)



Vita

Vernon Raymond Koym was born 17 August 1951 at Sinton, Texas. He graduated from Callalen High School in Corpus Christi, Texas in 1969. He attended Texas A&M University from which he graduated with a Bachelor of Science degree in Physics in 1973. Upon graduation, he was commissioned in the United States Air Force through the ROTC program at Texas A&M. He entered the AFIT School of Engineering in June 1979. He is married to the former Daria Lynn Starks.

Permanent Address: Box 121A, Route 6
Prescott, Arkansas

UNCLASSIFIED

SECURITY CLASSIFICATION OF THIS PAGE (When Data Entered)

| REPORT DOCUMENTATION PAGE | | READ INSTRUCTIONS BEFORE COMPLETING FORM |
|---|---------------------------------------|---|
| 1. REPORT NUMBER AFIT/GEP/PII/80-5 | 2. GOVT ACCESSION NO. AD A0 94 964 | 3. RECIPIENT'S CATALOG NUMBER |
| 4. TITLE (and Subtitle) A GAS FLOW TUBE FOR SPECTROSCOPIC STUDIES | | 5. TYPE OF REPORT & PERIOD COVERED MS Thesis |
| | | 6. PERFORMING ORG. REPORT NUMBER |
| 7. AUTHOR(S) VERNON R. KOYM CAPT USAF | | 8. CONTRACT OR GRANT NUMBER(S) |
| 9. PERFORMING ORGANIZATION NAME AND ADDRESS Air Force Institute of Technology (AFIT-EN) Wright-Patterson Air Force Base OH | | 10. PROGRAM ELEMENT PROJECT, TASK AREA & WORK UNIT NUMBERS |
| 11. CONTROLLING OFFICE NAME AND ADDRESS | | 12. REPORT DATE December 1980 |
| 14. MONITORING AGENCY NAME & ADDRESS (if different from Controlling Office) | | 13. NUMBER OF PAGES 101 |
| | | 15. SECURITY CLASS. (of this report) UNCLASSIFIED 15a. DECLASSIFICATION/DOWNGRADING SCHEDULE |
| 16. DISTRIBUTION STATEMENT (of this Report) Approved for Public Release; Distribution Unlimited. | | |
| 17. DISTRIBUTION STATEMENT (of the abstract entered in Block 20, if different from Report) | | |
| 18. SUPPLEMENTARY NOTES Approved for Public Release; IAW AFR 190-17 FREDERICK C. LYNCH, Major, USAF Director of Public Affairs 06 JAN 1981 | | |
| 19. KEY WORDS (Continue on reverse side if necessary and identify by block number) Flow Tube Iodine Fast Flow Reactor Lead Chemiluminescence Lead Oxide | | |
| 20. ABSTRACT (Continue on reverse side if necessary and identify by block number) A gas flow tube was constructed to allow chemical reaction studies at pressures from 0.1 torr to 30 torr. The tube was designed to allow introduction of oxidants, diluents, or excited gases. A furnace was constructed to produce high temperature vapor in the combustion chamber of the flow tube. The flow tube was characterized by its pumping speed, pressure, throughput, and evaluating Reynolds and Knudsen numbers at (Continued on Reverse) | | |

UNCLASSIFIED

SECURITY CLASSIFICATION OF THIS PAGE(When Data Entered)

BLOCK 20: Abstract (Cont'd)

pressures from 0.1 - 20 torr. Two experiments were conducted to verify the flow tube performance. Singlet molecular oxygen was produced in a microwave discharge and reacted with gaseous I_2 to yield chemiluminescence from the transition $I_2(B) \rightarrow I_2(A)$.

The spectrum was recorded and the bandheads assigned to vibrational transitions predicted by theory. PbO was created by reacting vaporized lead with N_2O . The emissions were compared with literature.

UNCLASSIFIED

